Heterometallic Clusters Derived from the Unsaturated Carbyne-Bridged Dimolybdenum Complexes $[Mo_2(\eta^5\text{-}C_5H_5)_2(\mu\text{-}CPh)(\mu\text{-}PCy_2)(CO)_x]$ (x = 1, 2).

M. Ángeles Alvarez, M. Esther García, Sonia Menéndez, and Miguel A. Ruiz*

Departamento de Química Orgánica e Inorgánica/IUQOEM, Universidad de Oviedo, E-33071 Oviedo, Spain.

Abstract

The carbonyl-bridged complex $[Mo_2Cp_2(\mu\text{-}CPh)(\mu\text{-}PCy_2)(\mu\text{-}CO)]$ (**1**) reacted with $[Fe_2(CO)_9]$ at room temperature to give the 46-electron trinuclear cluster $[FeMo_2Cp_2(\mu_3\text{-}CPh)(\mu\text{-}PCy_2)(CO)_5]$ (Mo–Mo = 2.6782(4) Å), and a similar Mo_2Ru cluster was obtained upon reaction with $[Ru_3(CO)_{12}]$ under irradiation with visible-UV light (Cp = η^5-C_5H_5). Compound **1** reacted with $[Co_2(CO)_8]$ at room temperature to give the 60-electron tetrahedral cluster $[Co_2Mo_2Cp_2(\mu_3\text{-}CPh)(\mu\text{-}PCy_2)(CO)_7]$, which in solution exits as an equilibrium mixture of two isomers and presumably displays phosphide and carbyne ligands in a cisoid arrangement. This compound evolved thermally to give a third isomer having these ligands arranged in a transoid way (P–Mo–C = 126.3(1)^o, Mo–Mo = 2.9612(6) Å). The dicarbonyl complex $[Mo_2Cp_2(\mu\text{-}CPh)(\mu\text{-}PCy_2)(CO)_2]$ (**2**) reacted with $W(CO)_6$ under visible-UV light irradiation to give two thermally unstable isomers of the 46-electron trinuclear cluster $[Mo_2WCp_2(\mu_3\text{-}CPh)(\mu\text{-}PCy_2)(CO)_6]$. Reaction of **2** with $[AuCl(PR_3)]$ (R = Me, p-tol, ^{i}Pr) in the presence of $TlPF_6$ gave first the corresponding cationic clusters *trans*-$[AuMo_2Cp_2(\mu_3\text{-}CPh)(\mu\text{-}PCy_2)(CO)_2(PR_3)]PF_6$, which then evolved thermally to the more stable isomers *cis*-$[AuMo_2Cp_2(\mu_3\text{-}CPh)(\mu\text{-}PCy_2)(CO)_2(PR_3)]PF_6$ (Mo–Mo = 2.810(1) Å for R = ^{i}Pr), selectively formed with a *syn* conformation of the carbyne and Cp ligands, except for the PMe_3 complex. In contrast, reaction of **2** with CuCl led to a cluster of composition $[CuMo_2ClCp_2(\mu_3\text{-}CPh)(\mu\text{-}PCy_2)(CO)_2]$, presumably present as a monomer in solution, but certainly appearing in the solid state as a centrosymmetric dimer held by bridging Cu–Cl–Cu interactions (Mo–Mo= 2.8004(5), Cu–Cl = 2.309(1), 2.409(1) Å).

Keywords: Molybdenum; Metal–metal interactions; Phosphorus ligands; Carbonyl complexes; Carbyne complexes; Heterometallic clusters.

1. Introduction

The chemistry of carbyne complexes is an extensively studied area within organometallic chemistry [1]. The reactivity of these complexes mainly stems from the metal–carbon multiple bonds present in these molecules, of highest order (three) for terminal ligands. Carbyne-bridged complexes have reduced metal–carbon bond orders (between one and two) and hence reduced reactivity; however, such reactivity can be significantly increased by the presence of metal–metal multiple bonds in the same molecule [2,3]. In this line of work, we recently initiated studies on the reactivity of the unsaturated benzylidyne-bridged complexes $[Mo_2Cp_2(\mu\text{-CPh})(\mu\text{-PCy}_2)(\mu\text{-CO})]$ (**1**) [4] and $[Mo_2Cp_2(\mu\text{-CPh})(\mu\text{-PCy}_2)(CO)_2]$ (**2**) [5] (Cp = η^5-C_5H_5) (Chart 1), which combine multiple Mo–Mo and Mo–C bonds and therefore provide a platform for the analysis of the synergic effect of these functionalities on their chemical behaviour.

Chart 1

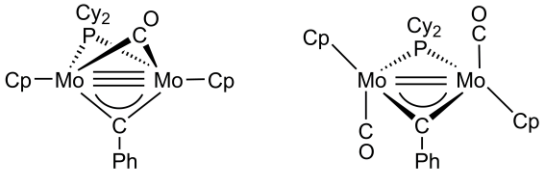

In preliminary studies on the behaviour of compounds **1** and **2**, we showed that both species display high reactivity under mild conditions towards many different reagents, usually involving participation of both the unsaturated dimetal centre and the carbyne ligand, whereby interesting C–C, C–P and C–H bond formation processes could be induced [4,5]. In this paper we explore reactions of compounds **1** and **2** with different metal complexes so as to examine their potential use in the rational synthesis of carbyne-bridged heterometallic clusters. This type of complexes was extensively studied by Stone and co-workers in the 80's. By using the isolobal analogy relating the C≡C bond of organic alkynes with the M≡C bond of mononuclear carbyne complexes, they synthesized a great variety of polynuclear complexes with bridging carbyne ligands starting from mononuclear complexes of type $[MCp(CR)(CO)_2]$ and related species [1d, 6]. In most cases, a change in the coordination mode of the carbyne ligand, from terminal to the μ_2 and μ_3 modes was observed. More recently we examined comparable reactions of the methoxycarbyne-bridged analogues of compounds **1** and **2**, which indeed proved to be useful reagents to prepare different trinuclear and tetranuclear clusters [7, 8]. As it will be shown below, complexes **1** and **2** are nucleophilic enough to react with different precursors of unsaturated metal fragments of type $M(CO)_x$ (M = W, Fe, Ru, Co), whereby different tri- and tetranuclear heterometallic clusters can be obtained, all having the benzylidyne ligand bound to three metal centres. Complex **2**

proved to be even more reactive than monocarbonyl **1**, and it was able to add $[Au(PR_3)]^+$ or CuCl units, to yield heterometallic derivatives with Mo_2Au and Mo_2Cu metal cores.

2. Results and Discussion

*2.1. Addition of 16-electron metal fragments to complex **1**.*

The 16-electron fragments $MnL(CO)_2$ (L = Cp, η^5-C_5H_4Me) can be generated *in situ* through photolysis of the corresponding precursors $[MnL(CO)_3]$. Unfortunately, the photolysis of compound **1** in presence of these complexes only rendered partial transformation of **1** into its ketenyl derivative $[Mo_2Cp_2\{\mu\text{-}C(Ph)CO\}(\mu\text{-}PCy_2)(CO)_2]$ [3]. This is obviously due to reaction of **1** with the carbon monoxide generated by the photolytic process, and is in contrast with the behaviour of the related methoxycarbyne-bridged complex $[Mo_2Cp_2(\mu\text{-}COMe)(\mu\text{-}PCy_2)(\mu\text{-}CO)]$, which gave the trinuclear complexes $[Mo_2MnCp_2L(\mu\text{-}COMe)(\mu\text{-}PCy_2)(CO)_4]$ under similar conditions [7]. In contrast, compound **1** reacts at room temperature with $[Fe_2(CO)_9]$, or with $[Ru_3(CO)_{12}]$ under visible-UV irradiation, to give the corresponding trinuclear clusters $[Mo_2MCp_2(\mu_3\text{-}CPh)(\mu\text{-}PCy_2)(CO)_5]$ [M = Fe (**3a**), Ru (**3b**)] (Scheme 1), in a process paralleling that of its methoxycarbyne-bridged analogue. These clusters formally follow from addition of 16-electron $M(CO)_4$ fragments to compound **1**, with further shift of one carbonyl ligand from the added fragment to the Mo_2 centre.

Scheme 1

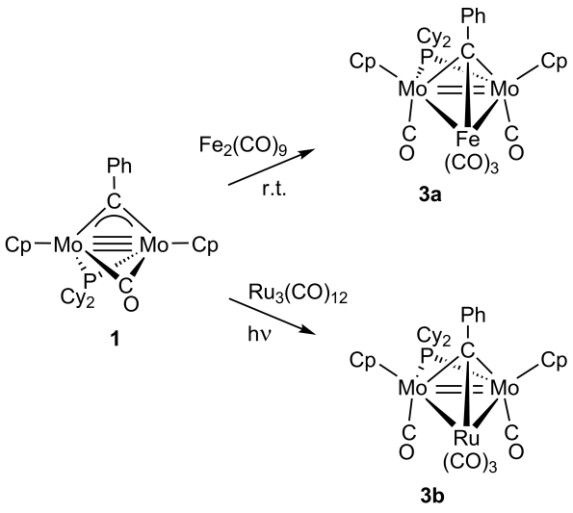

Attempts to add 16-electron fragments of the group 6 metals upon photolysis of mixtures of **1** and the carbonyl complexes $[M(CO)_6]$ (M = Mo, W) failed to give detectable amounts of new heterometallic clusters, which is surprising when recalling our previous synthesis of the methylidyne-bridged trinuclear cluster $[Mo_3Cp_2(\mu_3\text{-}CH)(\mu\text{-}PCy_2)(CO)_7]$ upon photolysis of the methyl complex $[Mo_2Cp_2(\mu\text{-}CH_3)(\mu\text{-}$

$PCy_2)(CO)_2]$ and $[Mo(CO)_6]$ [9]. This difference might be in part explained by the relatively important steric demands of the benzylidyne ligand, which might disfavour the approach of fragments needed for cluster formation, thus imposing a kinetic barrier to the reaction. In line with this, we note that the dicarbonyl complex **2**, with a more accessible dimetal centre, is able to form a new Mo_2W cluster, if unstable, under similar conditions, as discussed later.

*2.2. Solid-state structure of complex **3a**.*

The molecule of **3a** (Figure 1 and Table 1) is built from two MoCp(CO) and one $Fe(CO)_3$ fragment defining a triangular metal core bridged by PCy_2 (on the Mo_2 edge) and benzylidyne (on the Mo_2Fe face) ligands. The Mo fragments are arranged in a cisoid manner, with the cyclopentadienyl groups on the same side of the metal plane, and the carbonyl ligands on the opposite side, almost parallel to each other. The short Mo(1)–Mo(2) length of 2.6782(4) Å falls within the range expected for a double Mo–Mo bond and is very similar to the distance found in the isoelectronic (46-electron) methoxycarbyne-bridged cluster $[Mo_2FeCp_2(\mu_3\text{-}COMe)(\mu\text{-}PCy_2)(CO)_5]$ [2.688(3) Å] [7], which suggests that the electronic unsaturation of the molecule is localized on that bond. In agreement with this, the Mo–Fe distances of 2.7901(5) and 2.7555(5) Å are only slightly shorter than those measured in related, but electron-precise clusters such as $[FeMo_2Cp'_2(\mu_3\text{-}S)(CO)_7]$ (ca. 2.82 Å) [10] and $[FeMo_2Cp_2(\mu_3\text{-}PPh)(CO)_7]$ (ca. 2.92 Å) [11]. Yet, the Fe atom is formally unsaturated, with a local electron count of 17 electrons. This is consistent with the conformation of the Mo-bound carbonyls, which are directed towards the Fe atom in an incipient semibridging interaction that partially alleviates such unsaturation (C2···Fe ca. 2.66 Å). Finally we note that the carbyne ligand is symmetrically placed over the metal triangle (if we allow for the lower covalent radius of Fe) while the phosphide ligand on the Mo_2 edge is placed out of the plane defined by the metal atoms, away from the carbyne ligand (P–Mo–C3 ca. 103°), with the Mo_2Fe and Mo_2P planes defining an angle of ca. 153°.

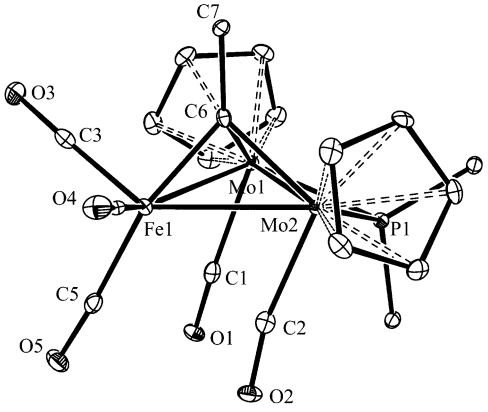

Figure 1. ORTEP diagram (25% probability) of one of the two independent molecules of compound **3a** in the crystal lattice, with Cy and Ph groups (except their C^1 atoms) omitted for clarity.

Table 1. Selected bond lengths (Å) and angles (°) for compound **3a**

Mo(1)–Mo(2)	2.6782(4)	Mo(2)–Mo(1)–Fe(1)	60.48(1)
Mo(1)–Fe(1)	2.7901(5)	Mo(1)–Mo(2)–Fe(1)	61.77(1)
Mo(2)–Fe(1)	2.7555(5)	Mo(2)–Mo(1)–C(1)	90.1(1)
Mo(1)–C(6)	1.123(3)	Mo(1)–Mo(2)–C(2)	93.2(1)
Mo(2)–C(6)	2.097(3)	Mo(1)–C(6)–Fe(1)	87.5(1)
Fe(1)–C(6)	1.908(3)	Mo(2)–C(6)–Fe(1)	86.8(1)
Mo(1)–C(1)	1.994(3)	P(1)–Mo(1)–C(1)	86.7(1)
Mo(2)–C(2)	1.998(3)	P(1)–Mo(2)–C(2)	94.1(1)
Fe(1)–C(3)	1.762(4)	P(1)–Mo(1)–C(6)	102.8(1)
Fe(1)–C(4)	1.761(3)	P(1)–Mo(2)–C(6)	103.5(1)
Fe(1)–C(5)	1.817(3)	P(1)–Mo(1)–Mo(2)–Fe(1)	153.04(3)

*2.3. Solution structure of complexes **3a** and **3b**.*

Spectroscopic data in solution for complexes **3a** and **3b** (Table 2) are very similar to each other and fully consistent with the structure found in the crystal for **3a**. The IR spectra in solution for both compounds display three strong C–O stretching bands, with the frequencies and intensities expected from a pyramidal $M(CO)_3$ fragment [12]. Similar IR patterns were observed for the methoxycarbyne-bridged analogues of compounds **3** [7], or for the related alkynyl-bridged cluster $[FeMo_2Cp_2(\mu\text{-}PPh_2)(\mu_3\text{-}\eta^2\text{-}CCPh)(CO)_5]$ [13]. In contrast, the carbonyl ligands bound to molybdenum gave rise to very weak absorptions hardly hinted in the spectrum baseline, a common circumstance in this kind of heterometallic clusters.

Table 2. Selected IR and NMR data for new compounds

Compound	ν(CO)[a]	δ(P)[b]	δ(μ-C){J_{CP}}[b]
$[Mo_2Cp_2(\mu\text{-CPh})(\mu\text{-PCy}_2)(\mu\text{-CO})]$ (**1**)[c]	1686 (s)	228.5	385.2 {15}
$[Mo_2Cp_2(\mu\text{-CPh})(\mu\text{-PCy}_2)(CO)_2]$ (**2**)[c]	1913 (w, sh), 1895 (vs)	117.6	428.4 {5}
$[Mo_2FeCp_2(\mu_3\text{-CPh})(\mu\text{-PCy}_2)(CO)_5]$ (**3a**)	2012 (vs), 1947 (s), 1924 (m)	178.6	306.9
$[Mo_2RuCp_2(\mu_3\text{-CPh})(\mu\text{-PCy}_2)(CO)_5]$ (**3b**)	2031 (vs), 1968 (s), 1941 (m), 1887 (w), 1843 (vw)	178.8	286.7
$[Co_2Mo_2Cp_2(\mu_3\text{-CPh})(\mu\text{-PCy}_2)(CO)_7]$ (**4**)	2014 (s), 1970 (vs), 1887 (w), 1850 (w), 1818 (w), 1759 (w)	316.9 (A) 347.2 (B)[d,e]	309.3 (A)[d]
$[Co_2Mo_2Cp_2(\mu_3\text{-CPh})(\mu\text{-PCy}_2)(CO)_4(\mu\text{-CO})_3]$ (**5**)	2004 (m), 1978 (vs), 1965 (sh), 1906 (m), 1826 (w), 1777 (w), 1760 (w).	376.2	302.4 {18}
$[Mo_2WCp_2(\mu_3\text{-CPh})(\mu\text{-PCy}_2)(CO)_6]$ (**6**)	2020 (m), 1951 (s), 1928 (s), 1873 (m, br)[f]	177.3 (*cis*), 158.0 (*trans*)[g]	300.5 (*cis*)[h]
trans-$[AuMo_2Cp_2(\mu_3\text{-CPh})(\mu\text{-PCy}_2)(CO)_2(PMe_3)](PF_6)$ (**7a**)	1943 (w), 1910 (vs)	160.1, 17.3[h]	377.0 {25}[h]
trans-$[AuMo_2Cp_2(\mu_3\text{-CPh})(\mu\text{-PCy}_2)(CO)_2\{P(p\text{-tol})_3\}](PF_6)$ (**7b**)	1944 (w), 1913 (vs)	168.9, 53.4	
trans-$[AuMo_2Cp_2(\mu_3\text{-CPh})(\mu\text{-PCy}_2)(CO)_2(P^iPr_3)](PF_6)$ (**7c**)	1943 (w), 1910 (vs)	171.7, 84.1[h]	370.0 {19}[h]
cis-$[AuMo_2Cp_2(\mu_3\text{-CPh})(\mu\text{-PCy}_2)(CO)_2(PMe_3)](PF_6)$ (**8a**)	1944 (vs), 1904 (w)	217.1, 29.8 (*anti*) 223.8, 29.8 (*syn*)[i]	348.3 {26} (*anti*)
cis-$[AuMo_2Cp_2(\mu_3\text{-CPh})(\mu\text{-PCy}_2)(CO)_2\{P(p\text{-tol})_3\}](PF_6)$ (**8b**)	1948 (vs), 1906 (w)	222.4, 63.8	
cis-$[AuMo_2Cp_2(\mu_3\text{-CPh})(\mu\text{-PCy}_2)(CO)_2(P^iPr_3)](PF_6)$ (**8c**)	1946 (vs), 1903 (w)	223.5, 92.6	346.6 {25}
$[CuMo_2ClCp_2(\mu_3\text{-CPh})(\mu\text{-PCy}_2)(CO)_2]$ (**9**)	1938 (vs), 1894 (w)	202.7	349.2

[a] Recorded in CH_2Cl_2 solution, data in cm^{-1}.
[b] Recorded at room temperature in CD_2Cl_2 solution at 161.97 (^{31}P) and 100.61 MHz (^{13}C), unless otherwise stated; δ in ppm relative to external 85% aqueous H_3PO_4 and tetramethylsilane, respectively, with C-P coupling constants {J_{CP}} in Hz; all cationic complexes also displayed a ^{31}P resonance due to anion PF_6^- at −144.6 ppm (septet, J_{PF} = 713 Hz).
[c] data taken from reference 3
[d] Recorded at 183 K.
[e] Ratio of isomers A/B ca. 2/1.
[f] Other C–O stretching bands of this compound might be obscured by that of excess $[W(CO)_6]$ invariably present in the reaction mixtures (see text).
[g] Recorded at 233 K, ratio of isomers *cis*/*trans* ca. 5/4.
[h] Recorded at 233 K.
[i] Ratio of isomers *syn*/*anti* ca. 1/5.

The ^1H and ^{13}C NMR data for compounds **3** reveal the presence of an effective symmetry plane relating the chemical environment of both Mo fragments, evidenced by the appearance of single resonances for the Cp ligands. The molybdenum-bound carbonyl ligands give rise to a quite deshielded ^{13}C resonance at 249.8 ppm (**3a**) and 253.0 ppm (**3b**), which suggests an incipient semibridging character, in agreement with the structure of **3a** in the crystal. In contrast, the iron- and ruthenium-bound carbonyls give rise in each case to a single resonance in the region of terminal carbonyls, thus revealing the operation of a dynamic process, fast on the NMR time scale, effectively exchanging the chemical environments of the three carbonyl ligands bound to the group 8 metal in each case, a common circumstance for di- and polynuclear carbonyl complexes having pyramidal $M(CO)_3$ units. As for the carbyne ligand, its ^{13}C resonance

(306.9 ppm for **3a** and 286.7 ppm for **3b**) is considerably more shielded than those of the binuclear precursors **1** and **2** (Table 2), consistent with the change in coordination mode operated on the carbyne ligand (from μ_2 to μ_3) upon formation of these clusters. Finally, the $^{31}P\{^1H\}$ NMR spectrum of complexes **3a** and **3b** displays in each case a relatively deshielded resonance at ca. 179 ppm, a shift very close to those of their methoxycarbyne-bridged analogues (ca. 182 ppm) [7] or the isoelectronic methylidyne-bridged cluster $[Mo_2RuCp_2(\mu_3\text{-}CH)(\mu\text{-}PCy_2)(CO)_5]$ (180.9 ppm) [14]. Unexpectedly, the room temperature ^1H NMR spectra of complexes **3** displayed broad (**3a**) or undetectable (**3b**) resonances for the *ortho* H atoms of the phenyl ring. Upon cooling the corresponding solutions, these resonances eventually appeared split and separated from each other by some 3 ppm (1200 Hz). This is indicative of slow rotation of the phenyl group in both compounds, which at room temperature would only approach the fast exchange limit for the closer *meta* resonances, while the more separated *ortho* resonances would be in a region close to coalescence at room temperature, even disappearing into the baseline of the spectrum due to their very different resonance frequency [15].

Scheme 2

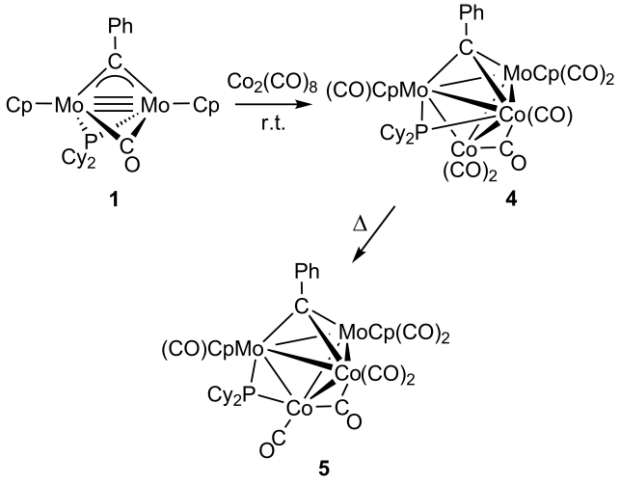

*2.4. Reactions of compound **1** with $[Co_2(CO)_8]$.*

Compounds having triple bonds between metal and carbon atoms may react with binuclear carbonyl complexes having metal–metal triple bonds to give heterometallic derivatives exhibiting trimetallatetrahedrane central cores [16]. We wondered if complex **1**, with a metal–metal triple bond, might undergo similar reactions to give tetranuclear derivatives exhibiting tetrahedral metal cores. Unfortunately, no reaction was observed between **1** and the triply bonded tetracarbonyl $[Mo_2Cp_2(CO)_4]$, either under thermal (in refluxing toluene solution) or photochemical activation (under visible-UV light irradiation), a process perhaps prevented by the relatively high steric demands of the dimetal centre in **1**, already noticed. In contrast, reaction with $[Co_2(CO)_8]$ takes

place readily in toluene solution at room temperature to give selectively the tetranuclear cluster $[Co_2Mo_2Cp_2(\mu_3\text{-}CPh)(\mu\text{-}PCy_2)(CO)_7]$ (**4**) (Scheme 2), which follows from formal addition of a triply-bonded $Co_2(CO)_6$ unit to compound **1** to build a Mo_2Co_2 tetrahedron, with further rearrangement of phosphide and carbonyl ligands. Compound **4** is thermally unstable in solution, and rearranges when stirred in toluene at room temperature for 10 h, or when heated at 343 K for 3 h, to give quantitatively the isomer $[Co_2Mo_2Cp_2(\mu_3\text{-}CPh)(\mu\text{-}PCy_2)(CO)_4(\mu\text{-}CO)_3]$ (**5**), a cluster differing from **4** in the relative disposition of the bridging carbyne and PCy_2 ligands, and in the arrangement of carbonyls.

Cluster **4** in turn exists in solution as a mixture of two interconverting isomers **A** and **B** of similar spectroscopic properties (Table 2 and Experimental section), with their equilibrium ratio being ca. 2/1 at 183 K. In fact, the room temperature $^{31}P\{^1H\}$ NMR spectrum of **4** displays just a broad resonance at 329 ppm, with the large line width of this resonance being only in part attributable to scalar coupling to a quadrupolar nucleus as ^{59}Co (100% natural abundance) [17]. Indeed, upon cooling of the solution, this resonance further broadened and eventually split below 213 K, to give separate resonances at 316.9 (isomer **A**) and 347.2 ppm (isomer **B**), with relative intensities 2:1. Parallel changes could be appreciated in the low temperature ^1H and $^{13}C\{^1H\}$ NMR spectra of compound **4**, which at room temperature displayed two averaged cyclopentadienyl resonances, each splitting into two resonances of ca. 2:1 relative intensities at low temperature (see the Experimental section). The low temperature $^{13}C\{^1H\}$ NMR spectrum of **4** displays a carbyne resonance for the major isomer at 309.3 ppm, indicative of a μ_3-coordination, but we could not identify the corresponding resonance for the minor isomer nor we could identify all carbonyl resonances, therefore we cannot be precise about the structural differences in these isomers, possibly derived from distinct arrangements of the Mo-bound carbonyl ligands, perhaps essentially terminal in one isomer, and including bridging or semibridging ones in the other one (**T** and **P** in Scheme 3). The IR spectrum of **4** would be consistent itself with many different structures, since it displays two very strong bands in the characteristic range of terminal CO ligands bound to Co, along with several bands of lower intensity and frequency consistent with the presence of Mo-bound terminal and semibridging carbonyls, or Co-bound bridging ligands.

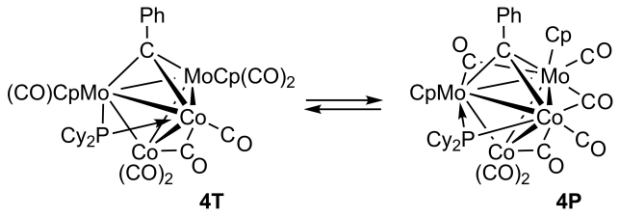

Scheme 3. Proposed structures for the interconverting isomers of compound **4**.

The ^{31}P chemical shifts of both isomers of **4** are unusually high when compared to the values commonly found in complexes with PCy_2 ligands bridging two Mo atoms, and still substantially higher than those measured in trinuclear complexes displaying PR_2 ligands over Mo–Co edges (cf. 196.4 ppm in $[Co_2MoCp\{\mu_3\text{-}C(C_6H_4Me)\}(\mu\text{-}H)(\mu\text{-}PPh_2)(CO)_6]$ [18], or 220 ppm in $[FeMoCo(\mu_3\text{-}CCPh)(\mu\text{-}PPh_2)(CO)_6]$ [12]). We attribute this unusual deshielding of the P nucleus in **4** to a particularly strong cluster effect in this tetranuclear molecule. Indeed, it has been shown previously that upon increasing the nuclearity of some PR_2-bridged clusters there is a general increase in the ^{31}P chemical shifts, an effect attributed to the progressive decrease of the HOMO–LUMO gap in the corresponding clusters [19].

*2.5. Structure of compound **5**.*

The molecule of **5** in the crystal (Figure 2 and Table 3) is built on a Mo_2Co_2 tetrahedral core, with the benzylidyne ligand symmetrically bridging the Mo_2Co1 face, the PCy_2 ligand bridging the Mo1–Co2 edge and a carbonyl ligand bridging the Co–Co edge in a slightly asymmetric way, with the average Co–C bond lengths of ca. 2.0 Å, being slightly longer than those in the binuclear complex $[Co_2Cp_2(\mu\text{-}CO)_2(\mu\text{-}C_3H_6)]$ [20]. The Co1 atom bears two terminal carbonyls, while Co2 is bound to the PCy_2 ligand and a terminal carbonyl, and is also involved in two weaker interactions with the Mo2-bound carbonyls (Co–C = 2.176(4), 2.254(4) Å). The Mo–C–O angles of ca. 155^o identify these ligands as bent-semibridging ones, under the classification by Crabtree and Lavin [21]. As for the PCy_2 ligand, its binding to the metal atoms (Mo–P = 2.432(1), Co–P = 2.194(1) Å) can be considered as essentially symmetrical if we bear in mind the large difference of ca. 0.28 Å between the covalent radii of Mo and Co [22]. Compound **5** can be classified as an electron-precise (60-electron) tetrahedral cluster, therefore all intermetallic lengths should be described as single bonds, in agreement with the measured distances of 2.62-2.79 (Mo–Co), 2.4932(7) (Co–Co) and 2.9612(6) Å (Mo–Mo) in the different edges of the tetrahedral core. All these lengths are comparable to those measured in other crystallographically characterized complexes having this sort of intermetallic bonds [23], particularly with those in the methoxycarbyne-bridged analogue of **5** ($[Co_2Mo_2Cp_2(\mu_3\text{-}COMe)(\mu\text{-}PCy_2)(CO)_4(\mu\text{-}CO)_3]$ [7]).

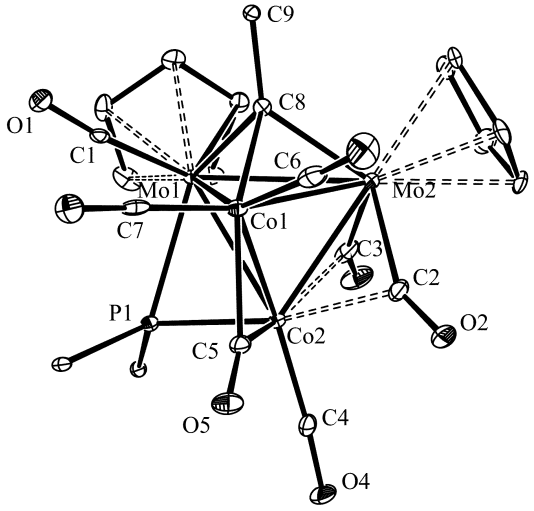

Figure 2. ORTEP diagram (25% probability) of compound **5**·CH_2Cl_2, with Cy and Ph groups (except their C^1 atoms) omitted for clarity.

Table 3. Selected bond lengths (Å) and angles (°) for compound **5**·CH_2Cl_2.

Mo(1)–Mo(2)	2.9612(6)	Mo(2)–C(2)	2.023(4)
Mo(1)–Co(1)	2.7681(6)	Mo(2)–C(3)	1.982(4)
Mo(1)–Co(2)	2.7903(7)	Co(2)–C(2)	2.176(4)
Mo(2)–Co(1)	2.7172(6)	Co(2)–C(3)	2.254(4)
Mo(2)–Co(2)	2.6247(7)	Co(2)–C(4)	1.756(4)
Co(1)–Co(2)	2.4932(7)	Co(2)–C(5)	1.877(4)
Mo(1)–C(8)	2.140(3)	Co(2)–P(1)	2.194(1)
Mo(2)–C(8)	2.118(4)	Co(1)–C(5)	2.034(4)
Co(1)–C(8)	1.960(3)	Co(1)–C(6)	1.760(4)
Mo(1)–C(1)	1.952(4)	Co(1)–C(7)	1.776(4)
Mo(1)–P(1)	2.432(1)	C(8)–C(9)	1.487(5)
Mo(1)–C(8)–Mo(2)	88.1(1)	C(5)–Co(1)–C(6)	101.7(2)
Mo(1)–C(8)–Co(1)	84.8(1)	C(6)–Co(1)–C(7)	96.0(2)
Mo(2)–C(8)–Co(1)	83.5(1)	P(1)–Co(2)–C(4)	98.4(1)
Co(2)–C(5)–Co(1)	79.1(1)	P(1)–Co(2)–C(5)	95.4(1)
P(1)–Mo(1)–C(1)	95.0(1)	C(4)–Co(2)–C(5)	96.5(2)
P(1)–Mo(1)–C(8)	126.3(1)	Mo(2)–C(2)–O(2)	154.2(3)
C(2)–Mo(2)–C(3)	89.7(2)	Mo(2)–C(3)–O(3)	156.8(4)

Spectroscopic data in solution for complex **5** at room temperature are not fully consistent with the asymmetric structure found in the crystal, since the ^1H and $^{13}C\{^1H\}$ NMR spectra rather point to an apparent equivalence of the Cp ligands of the molecule. Upon cooling of the solution, however, the cyclopentadienyl resonance in these spectra broadens and eventually splits into two distinct resonances of equal intensity, now in agreement with the structure found in the crystal (see the Experimental section). All of this indicates the operation in solution of a fluxional process generating an effective symmetry plane relating the Mo fragments of the molecule, likely involving a shift of the phosphide ligand between Mo atoms, balanced by a carbonyl shift in the opposite direction (Scheme 4).

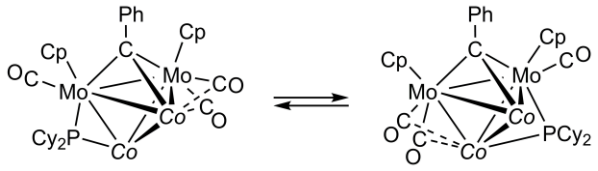

Scheme 4. Fluxional process proposed for compound **5**, with Co-bound carbonyls omitted for clarity.

The $^{31}P\{^{1}H\}$ NMR spectrum of **5** at room temperature displays a broad resonance at 376.2 ppm, with a broadening now attributable only to the presence of the quadrupolar ^{59}Co nucleus. Indeed, upon lowering of the temperature, the line width of this resonance was reduced due to the increased relaxation rate of the quadrupolar nucleus, but no splitting occurred. The IR spectrum of **5** in dichloromethane displays three very strong bands at 2004, 1978 and 1906 cm^{-1} consistent with the presence of three terminal Co-bound carbonyls in the molecule, along with other less intense absorptions at lower frequencies indicative of the retention of bridging and semibridging carbonyls in solution. Indeed the $^{13}C\{^{1}H\}$ NMR spectrum of **5** at 183 K displayed seven carbonyl resonances, consistent with the asymmetry of the static structure. Out of these, the most deshielded resonance (262.7 ppm) can be safely assigned to the ligand bridging the Co atoms, this being followed by the semibridging carbonyls between Co and Mo atoms (254.3 and 249.8 ppm), then a single terminal ligand bound to Mo (230.0 ppm) and finally three poorly deshielded resonances corresponding to the inequivalent terminal carbonyls bound to Co atoms (208.2, 205.0 and 199.6 ppm). The carbyne ligand gives rise to a resonance (δ_C 302.6 ppm) much more shielded than that of its precursor **1**, consistent with its coordination over three metal centres, and with a chemical shift comparable to that of its isomer **4**.

*2.6. Addition of metal fragments to dicarbonyl complex **2**.*

In a preliminary study we showed that the unsaturated benzylidyne complex **2** displayed a multisite reactivity on its central Mo_2PC core, involving addition of a wide variety of electron donors, but also simple acceptors such as the proton itself [5]. Therefore, this complex should to be potentially able to add different unsaturated metal fragments to give heterometallic clusters. Thus we examined reactions of **2** analogous to those discussed above for compound **1**. First we tested the photochemical reactions of **2** with the manganese complexes $[MnL(CO)_3]$ (L = Cp, η^5-C_5H_4Me), but no new clusters were formed, with **1** and the known ketenyl derivative $[Mo_2Cp_2\{\mu\text{-}C(Ph)CO\}(\mu\text{-}PCy_2)(CO)_2]$ [3], being the only new species being detected in the corresponding reaction mixtures, thus reproducing the behaviour of monocarbonyl **1**. On the other hand, complex **2** reacted with $[Fe_2(CO)_9]$, $[Ru_3(CO)_{12}]$ and $[Co_2(CO)_8]$ to give the same heterometallic clusters (**3**, **4** and **5**) obtained from **1**. Compound **2**, however, was able to add other fragments that failed to be incorporated to monocarbonyl **1**, this including the

tungsten fragment $W(CO)_5$ and the group 11 metal fragments $[AuPR_3]^+$ and CuCl, next discussed.

*2.7. Addition of 16-electron $M(CO)_5$ fragments to complex **2**.*

The photochemical reaction of **2** with $[Mo(CO)_6]$ led to a mixture of monocarbonyl **1** and the ketenyl complex $[Mo_2Cp_2\{\mu\text{-}C(Ph)CO\}(\mu\text{-}PCy_2)(CO)_2]$, obviously formed as a result of the unavoidable carbonylation/decarbonylation processes taking place under the experimental conditions. In contrast, reaction with $[W(CO)_6]$ at 263 K yielded the cluster $[Mo_2WCp_2(\mu_3\text{-}CPh)(\mu\text{-}PCy_2)(CO)_6]$ (**6**) as the major product, along with variable amounts of **1** and its ketenyl derivative. Compound **6** was generated as a mixture of two isomers presumably differing in the relative arrangement (*cis* or *trans*) of the carbonyls in the $Mo_2(CO)_2$ subunit of the cluster (Chart 2), and the *cis/trans* ratio in the final mixture was dependent on the exact experimental conditions (temperature and time, particularly), being of ca. 5/4 after 90 min irradiation at 263 K. Since the carbonyl arrangement in the parent compound **2** is a transoid one (Chart 1), the above suggests that a *trans* to *cis* rearrangement takes place at significant extent under photolytic conditions. This is not an unusual rearrangement, and has been previously observed, for instance, in the structurally related diiron complex $[Fe_2Cp_2(\mu\text{-}H)(\mu\text{-}PPh_2)(CO)_2]$ [24]. In any case, both isomers of compound **6** are thermally unstable and decompose in solution at room temperature, to give **1** and $[W(CO)_6]$.

Chart 2

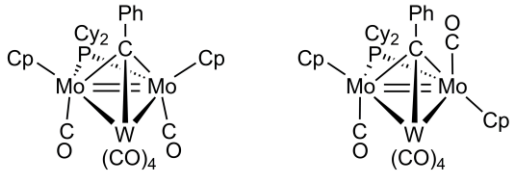

***cis*-6** ***trans*-6**

The structure proposed for the major isomer ***cis*-6** is comparable to that of the iron complex **3a** after replacement of the $Fe(CO)_3$ unit with the isoelectronic fragment $W(CO)_4$ (Chart 2). Indeed, these complexes share almost the same ^{31}P chemical shift of ca. 178 ppm. In agreement with such a proposal, this isomer displays a single NMR resonance for each pair of Cp and Mo-bound carbonyls (see the Experimental section), and its ^{13}C carbyne resonance at 300.5 ppm is indicative of a μ_3-coordination over a Mo_2W triangle. Unfortunately, no resonances for the W-bound carbonyls could be identified in the $^{13}C\{^1H\}$ NMR spectrum of the mixture of isomers even at low temperature. Yet, identification of the tungsten fragment in **6** as a tetracarbonyl (rather than pentacabonyl) fragment is soundly based on the fact that the IR spectrum of the reaction mixture displays its more energetic C–O stretch (the one expectedly arising from the symmetrical stretch of the $W(CO)_x$ fragment) at just 2020 cm^{-1}, a frequency

too low for a $W(CO)_5$ fragment, but of the correct magnitude for a $W(CO)_4$ fragment. For comparison, the $W(CO)_5$ fragment in the related heptacarbonyl clusters $[Mo_2WCp_2(\mu_3\text{-}CH)(\mu\text{-}PCy_2)(CO)_7]$ and $[Mo_2WCp_2(\mu_3\text{-}H)(\mu\text{-}PCy_2)(CO)_7]$ gives rise to a symmetric C–O stretch at 2041 and 2058 cm^{-1}, respectively [14, 25]. In contrast, the $W(CO)_4$ fragment in the structurally characterized cluster $[Mo_2WCp_2(\mu_3\text{-}P)(\mu\text{-}PCy_2)(\mu_3\text{-}PMe)(CO)_6]$ gives a symmetric C–O stretch at 2010 cm^{-1} [26], a figure much closer to that of compound **6**. The minor isomer ***trans*-6** is identified by a more shielded ^{31}P resonance at 158.0 ppm and, more significantly, because it displays two distinct ^{1}H and ^{13}C NMR cyclopentadienyl resonances. Unfortunately other relevant spectroscopic features of this isomer were obscured by the signals of the major isomer.

*2.8. Addition of $[Au(PR_3)]^+$ fragments to complex **2**.*

Because of the isolobal analogy relating the proton and gold(I) cations $[Au(PR_3)]^+$ [27], cationic gold fragments can be added to electron-rich complexes having metal–metal bonds to give heterometallic derivatives alike to the corresponding hydride complexes following from protonation [28]. Since dicarbonyl **2** is nucleophilic enough to be protonated [5], it could be anticipated that it should be able to add gold(I) cations, although the output of these reactions proved to be different from protonation.

Compound **2** reacts rapidly in dichloromethane solution with complexes $[AuCl(PR_3)]$, in the presence of $TlPF_6$, to give the corresponding cationic derivatives *trans*-$[AuMo_2Cp_2(\mu_3\text{-}CPh)(\mu\text{-}PCy_2)(CO)_2(PR_3)]PF_6$ [R = Me (**7a**), p-tol (**7b**), ^{i}Pr (**7c**)]. These products could not be isolated as pure materials. Moreover, they turned out to be thermally unstable, and progressively evolved at room temperature via a *trans* to *cis* rearrangement of the $Mo_2(CO)_2$ subunits, to yield the corresponding isomers *cis*-$[AuMo_2Cp_2(\mu_3\text{-}CPh)(\mu\text{-}PCy_2)(CO)_2(PR_3)]PF_6$ (**8a-c**) (Scheme 5). Although compounds **8** might in principle display two different isomers, depending on the relative orientation of the Cp and carbyne ligands (*syn* and *anti*), the available data for these products, to be discussed below, indicate that complexes bearing the bulkier Ph or ^{i}Pr groups are formed exclusively as the *syn* isomers, while the complex bearing the less bulky PMe_3 ligand displays both isomers, with the *anti* isomer being the major species in solution.

Spectroscopic data for the *trans* isomers **7** are similar to each other, indicating that they all share the same basic structure (Table 2 and Experimental section). They exhibit two C–O stretches in the IR spectrum, with the pattern (weak and strong, in order of decreasing frequency) characteristic of transoid $M_2(CO)_2$ oscillators [12]. A similar pattern was found in the carbene-bridged complex $[Mo_2Cp_2(\mu\text{-}\eta^1\text{:}\eta^2\text{-}CHPh)(\mu\text{-}PCy_2)(CO)_2]BF_4$ (actually one of the protonation products of **2** [5]), although the frequencies in **7** are lower, as expected from the lower electronegativity of the $AuPR_3$ groups (when compared to H).

Scheme 5

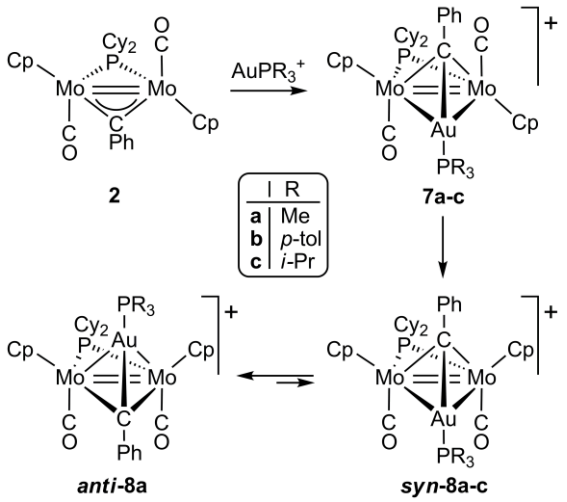

The $^{31}P\{^{1}H\}$ NMR spectra at 233 K of compounds **7a-c** display in each case three very different resonances: a quite deshielded singlet at around 165 ppm corresponding to the bridging dicyclohexylphosphide ligand, not far from the chemical shift of the *trans* isomer of **6**, another singlet in the 20 to 80 ppm region, in the typical range of phosphine ligands bound to Au(I) centres, and a characteristic septet at high field due to the counteranion PF_6^- (δ_P –144.6 ppm, J_{PF} = 713 Hz). The ^{13}C carbyne resonance in these products appears at ca. 375 ppm, a position considerably more shielded than that of the parent compound **2**, but less shielded than the corresponding resonances in compounds **3** to **6**, thus suggesting that interaction of the carbyne ligand with the gold atom perhaps is not very strong. Yet, the positioning of this ligand bridging over a Mo_2Au triangle (rather than terminally bound to the carbyne C atom, in a proton-like way) is further supported by the increased value of the two-bond P-C coupling (from 5 to 20-25 Hz), indicative of a reduction in the P–Mo–C angle upon complexation of the $AuPR_3$ fragment [29]. Finally, the inequivalence of both Mo centres in these isomers is evidenced by the presence of independent NMR resonances for the Cp groups in all cases.

2.9. Structure of the cis complexes 8.

Complexes **8** turned to be quite difficult to crystallize for diffraction purposes. Eventually, we were able to obtain a very few crystals of **8c**, and not of very high quality either. Moreover, they turned to correspond to a double salt of the same cation, of composition $[AuMo_2Cp_2(\mu_3\text{-}CPh)(\mu\text{-}PCy_2)(CO)_2(P^iPr_3)]_2(PF_6)(Cl)\cdot 1/2THF$, possibly formed thanks to the presence of residual chloride ions in the solution of the complex during crystallization. In spite of the poor quality of the diffraction data, however, the essential structural features of the cation in the crystal lattice are perfectly defined, although the metric accuracy is only moderate (Figure 3 and Table 4).

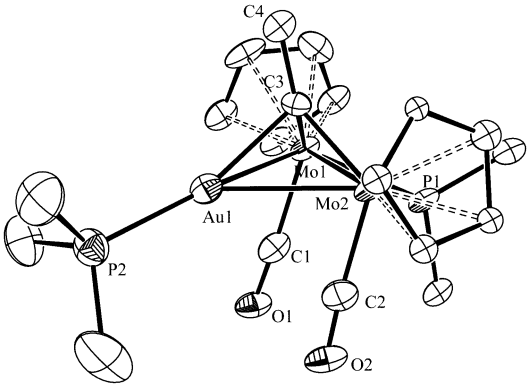

Figure 3. ORTEP diagram (25% probability) of the cation in compound **8c**, with Cy and Ph groups (except their C^1 atoms) omitted for clarity.

Table 4. Selected bond lengths (Å) and angles (°) for the cation in compound **8c**.

Mo(1)–Mo(2)	2.810(1)	Mo(1)–Au(1)–Mo(2)	58.48(3)
Mo(1)–Au(1)	2.883(1)	Mo(1)–P(1)–Mo(2)	71.12(9)
Mo(2)–Au(1)	2.869(1)	Mo(1)–C(3)–Mo(2)	86.9(5)
Mo(1)–P(1)	2.409(3)	P(1)–Mo(1)–C(3)	95.9(4)
Mo(2)–P(1)	2.422(3)	P(1)–Mo(2)–C(3)	95.3(5)
Mo(1)–C(1)	1.97(2)	P(1)–Mo(1)–C(1)	84.6(4)
Mo(2)–C(2)	1.97(2)	P(1)–Mo(2)–C(2)	83.9(4)
Mo(1)–C(3)	2.04(1)	P(2)–Au(1)–C(3)	160.9(3)
Mo(2)–C(3)	2.05(1)	Mo(1)–Mo(2)–C(2)	90.7(4)
Au(1)–C(3)	2.18(1)	Mo(2)–Mo(1)–C(1)	90.8(5)
Au(1)–P(2)	2.293(4)	P1–Mo1–Mo2–Au1	152.7(1)

The structure of the cation is built from two MoCp(CO) moieties arranged in a cisoid manner and a third fragment Au(P^iPr_3), thus defining a triangular Mo_2Au metal core bridged by a dicyclohexylphosphide ligand (over the Mo_2 edge) and a benzylidyne ligand (over the Mo_2Au triangle). The latter ligand and the Cp rings are placed on the same side of the intermetallic plane, therefore the cation corresponds to a *syn* isomer. The Mo(1)–Mo(2) distance of 2.810(1) Å is similar to the length of 2.8244(2) Å measured in the isoelectronic (but not isostructural) complex $[Mo_2AuCp_2(\mu\text{-}PEt_2)_2(CO)_2\{P(p\text{-}tol)_3\}]PF_6$ [8], and somewhat longer than that in the isoelectronic hydride $[W_2Cp_2(\mu\text{-}H)(\mu\text{-}PPh_2)(CO)_2]BF_4$ [2.7589(2) Å] [30], but still indicative of retention of considerable multiplicity in this bond. On the other hand, the Mo–Au distances of ca. 2.88 Å in **8c** are slightly longer than the values of ca. 2.82 Å measured in the mentioned Mo_2Au cluster, an effect possibly derived from the presence of the carbyne ligand face-bridging the metal triangle. In any case, all these values are within the range usually found in comparable tricentric Mo_2Au interactions (cf. 2.785(1) and 2.975(1) Å in $[Mo_2Cp_2(\mu\text{-}AuPPh_3)(\mu\text{-}PPh_2)(CO)_4]$ [31]). Finally, we note that the carbyne ligand might be viewed as bridging symmetrically the Mo_2Au triangle, since the corresponding lengths can be considered as comparable to each other [C–Mo = 2.04(1) and 2.05(1) Å; C–Au = 2.18(1)], after allowing for the ca. 0.18 Å lower

covalent radius of gold. As far as we know, there are no other structurally characterized complexes having a carbyne ligand triply-bridging a Mo_2Au or $MoAu_2$ triangle. In fact, the only other related compounds holding a comparable interaction involving gold atoms are the trimetal clusters $[AuPtWCp\{\mu_3\text{-}C(p\text{-}tol)\}(CO)_2(PMe_3)]^+$ [32] and $[AuCoW\{\mu_3\text{-}C(p\text{-}tol)\}(CO)_2(PPh_3)(\eta^6\text{-}C_2B_{10}H_{10}Me_2)]$ [33].

Spectroscopic data in solution for complexes **8b,c** (Table 2 and Experimental section) are similar to each other and fully consistent with the structure found for the double salt of **8c** in the crystal. They display a very similar ^{31}P phosphide resonance at ca. 223 ppm, some 50 ppm above the corresponding resonances of their *trans* isomers **7b,c**. This is a common trend when comparing ^{31}P chemical shifts of *cis* and *trans* isomers in other 32-electron dicarbonyl complexes, such as the bis(organophosphide) compounds $[Mo_2Cp_2(\mu\text{-}PR_2)(\mu\text{-}PR'_2)(CO)_2]$ (R = R' = Ph; R = Ph, R' = ^{t}Bu) [30, 34], or the cations $[Mo_2Cp_2\{\mu\text{-}\eta^2\text{:}\eta^2\text{-}C_2(OMe)_2\}(\mu\text{-}PCy_2)(CO)_2]BF_4$ [35]. The cisoid arrangement of the $Mo_2(CO)_2$ subunit in compounds **8b,c** is readily apparent from the relative intensity of the two C–O stretches in each case (strong and weak, in order of decreasing frequencies) [12], a circumstance also implying the presence of a symmetry plane bisecting the Mo_2Au triangle and relating both Mo fragments, this leading to a reduced number of ^1H and ^{13}C NMR resonances. We note that the carbyne resonance for **8c** displays a high P–C coupling of 25 Hz, consistent with the reduced P–Mo–C angle of ca. 95^o found in the crystal (cf. 105^o in the parent complex **2**); moreover its chemical shift of 346.6 ppm is 25 ppm lower than the corresponding shift in its *trans* isomer **7c**, thus indicating a substantially stronger interaction of the carbyne ligand with the gold atom in the more stable isomers **8**. This might be also a relevant factor defining the conformation of the $Mo_2(CO)_2$ subunit eventually observed in most heterometallic derivatives of compounds **1** and **2**. Finally, we also note that a conventional 2D NOESY spectrum of **8c** suggested spatial proximity of the Cp protons to the *ortho* protons of the phenyl ring of the cation, thus confirming the retention in solution of the *syn* geometry found for the cation of **8c** in the crystal.

As noted above, the PMe_3 complex **8a** displays two isomers in solution. These have very similar spectroscopic properties, in turn comparable to those of **8b,c**. The minor isomer displays a PCy_2 resonance at 223.8 ppm, a position almost identical to those of compounds **8b,c**, and is thus assigned to the isomer *syn*. The major isomer of **8a**, identified by a slightly more shielded ^{31}P resonance (δ_P 217.1 ppm) is therefore identified as the corresponding isomer *anti*, its prevalence being possibly facilitated by the smaller steric requirements of the $AuPMe_3$ fragment.

We should stress the fact that incorporation of $Au(PR_3)^+$ cations to dicarbonyl **2** follows a course different from protonation. In the latter reaction, the proton can be attached to the carbyne ligand (to give a carbene derivative) or to a Mo–PCy_2 bond (to

yield an agostic-like derivative $[Mo_2Cp_2(\mu\text{-}CPh)(\mu\text{-}PPh_2)(\mu\text{-}\kappa^1\text{:}\eta^2\text{-}PHCy_2)(CO)_2]^+$ [5]). This second route is obviously suppressed in the reactions of **2** with gold complexes, surely as a result of steric repulsions between the $Au(PR_3)$ fragments and the PCy_2 ligand, while the first route gives rise to a polycentric $Mo_2Au(\mu_3\text{-}CPh)$ interaction, rather than a single C–Au bond. The behaviour of **2** also differs from that of its methoxycarbyne-bridged analogue $[Mo_2Cp_2(\mu\text{-}COMe)(\mu\text{-}PCy_2)(CO)_2]$. The latter complex has been shown to react with $[AuCl\{P(p\text{-}tol)_3\}]$ under similar conditions, but the product obtained was the electron-precise tricarbonyl complex $[AuMo_2Cp_2(\mu_2\text{-}COMe)(\mu\text{-}PCy_2)(CO)_3\{P(p\text{-}tol)_3\}]PF_6$ a molecule proposed to be formed through initial attack of the gold electrophile to the Mo–P bond of the parent carbyne complex [8]. This exemplifies the great influence that subtle electronic and steric factors exert over the course of these cluster-building reactions.

*2.10. Reactions of complex **2** with CuCl.*

Compound **2** reacts with one equivalent of CuCl in dichloromethane solution at room temperature to give a cluster of formula $[CuMo_2ClCp_2(\mu_3\text{-}CPh)(\mu\text{-}PCy_2)(CO)_2]$ (**9**) (Chart 3). A single-crystal X-ray diffraction study revealed that in solid state this compound appears as a centrosymmetric dimer built from two molecules of **9** connected through Cu–Cl–Cu bridges (Figures 4 and 5, Table 5).

Chart 3

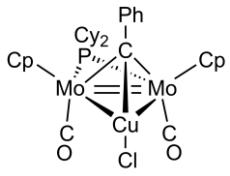

9

The asymmetric unit in the crystal (Figure 4) displays a Mo_2Cu triangle built from two cisoid MoCp(CO) fragments and a CuCl unit, with the PCy_2 ligand symmetrically bridging the Mo_2 edge, and the carbyne ligand triply bridging over the Mo_2Cu triangle. The phosphide ligand deviates from the metal plane away from the carbyne ligand (P–Mo–Mo–Cu ca. 152^o), in an identical extent to that found for complexes **3a** and **8c** (ca. 153^o). The metal-carbyne lengths are comparable to each other (Mo–C = 2.038(4), 2.048(4); Cu–C = 2.011(4) Å) which, by considering the smaller covalent radius of Cu (some 0.22 Å below that of Mo [22]), indicates a substantially weaker binding of the carbyne ligand to the copper atom. Yet, the Cu–C length in **9** is comparable to the value of 2.01(1) Å measured in the dimer $[WCuCp_2\{\mu\text{-}CN(Et)Me\}Cl(CO)_2]_2$ [36], even if the latter displays an edge-bridging (instead of face-bridging) carbyne ligand. As for the intermetallic distances, we note that the Mo–Mo separation of 2.8004(5) Å in **9** is only slightly shorter than the corresponding length in the isoelectronic complex **8c** [2.810(1) Å], indicating substantial multiplicity in that bond, while the Mo–Cu distances of ca.

2.76 Å are within the range expected for comparable polycentric bonds (cf. 2.78 Å in the tetranuclear cluster $[Cu_2Cl_2Mo_2Cp^*_2(\mu\text{-}S)_4]$ [37]).

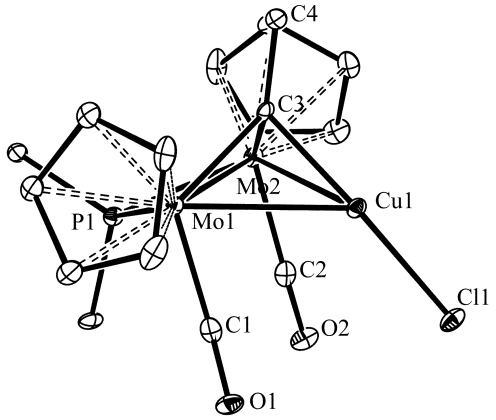

Figure 4. ORTEP diagram (25% probability) of the independent half-molecule of compound **9**·CH_2Cl_2, with Cy and Ph groups (except their C^1 atoms) omitted for clarity. The full molecule is shown in Figure 5.

Table 5. Selected bond lengths (Å) and angles (°) for compound **9**·CH_2Cl_2.

Mo(1)–Mo(2)	2.8004(5)	Mo(1)–P(1)–Mo(2)	70.95(3)
Mo(1)–Cu(1)	2.7565(6)	Mo(1)–Cu(1)–Mo(2)	61.06(1)
Mo(2)–Cu(1)	2.7560(6)	Mo(1)–C(3)–Mo(2)	86.5(1)
Mo(1)–P(1)	2.407(1)	Mo(2)–Mo(1)–C(1)	91.4(1)
Mo(2)–P(1)	2.418(1)	Mo(1)–Mo(2)–C(2)	91.4(1)
Mo(1)–C(1)	1.968(5)	P(1)–Mo(1)–C(1)	85.8(1)
Mo(2)–C(2)	1.977(5)	P(1)–Mo(2)–C(2)	83.7(1)
Mo(1)–C(3)	2.038(4)	P(1)–Mo(1)–C(3)	97.0(1)
Mo(2)–C(3)	2.048(4)	P(1)–Mo(2)–C(3)	96.4(1)
Cu(1)–C(3)	2.011(4)	Cu(1)–Cl(1)–Cu'(1)	94.25(4)
Cu(1)–Cl(1)	2.309(1)	Cl(1)–Cu(1)–Cl'(1)	85.75(4)
Cu(1)–Cl'(1)	2.409(1)	P1–Mo1–Mo2–Cu1	152.41(3)

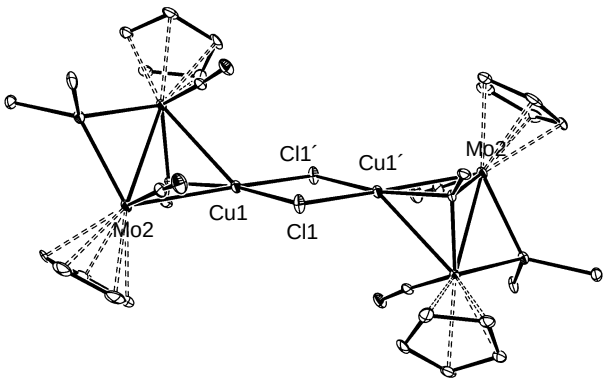

Figure 5. ORTEP diagram (25% probability) of the molecule of compound **9**·CH_2Cl_2 in the crystal lattice, with Cy and Ph groups (except their C^1 atoms) omitted for clarity.

As noted above, the asymmetric Mo_2Cu subunits in the crystal lattice are connected pair-wise so that the terminal chloride on a copper atom (Cu–Cl = 2.309(1) Å) binds the copper atom of the second Mo_2Cu subunit (Cu´–Cl = 2.409(1) Å) and vice versa, defining a Cu_2Cl_2 rhomboid placed on an inversion centre that relates the identical Mo_2Cu subunits (Figure 5). This sort of dimerization is common in CuCl derivatives

and follows from the general trend of Cu(I) complexes to reach coordination numbers of 4 or above, and was previously found also in the mentioned carbyne-bridged complex $[WCuCp_2\{\mu\text{-}CN(Et)Me\}Cl(CO)_2]_2$ (Cu–Cl = 2.307(4), 2.324(4) Å) [36]. In any case, the lengths involving the bridging chloride ligands are expectedly longer than those corresponding to terminal Cu–Cl bonds (cf. 2.162(1) Å in $[Mo_2CuClCp_2(\mu\text{-}\kappa^1\text{:}\kappa^1\text{:}\kappa^1\text{:}\eta^6\text{-}PMes^*)(CO)_2]$ [38]). We should note that the dimerization occurred in the case of **9** renders an unusual, square pyramidal-like, coordination environment around the Cu atom, with the carbyne and Mo2 atoms almost placed in the Cu_2Cl_2 plane. Currently we are unsure if this unusual geometry follows from genuine bonding interactions or from weak packing forces in the crystal lattice. Finally, it is worth mentioning that, even if addition of group 11 monohalides to carbyne complexes has been performed in the past to synthesize heterometallic clusters [36, 39], no copper derivatives with a face-bridging carbyne ligand could be crystallographically characterized, so complex **9** appears to be the first example in such a category.

Spectroscopic data for **9** in solution are in agreement with the structure of the Mo_2Cu subunits found in the crystal. The IR spectrum in dichloromethane displays two C–O stretching bands at 1938 (vs) and 1894 (w) cm^{-1}, with the typical pattern of cisoid $M_2(CO)_2$ oscillators, as found for the most stable isomers of the gold clusters discussed above. In agreement with this, the ^1H and $^{13}C\{^1H\}$ NMR spectra display a single resonance for the equivalent Cp groups. The carbyne ligand gives rise to a ^{13}C resonance 349.2 ppm, ca. 80 ppm more shielded than the corresponding resonance in the parent complex **2** and therefore consistent with the retention of the μ_3-bridging mode in solution. Similar chemical shifts have been previously found in related Cu clusters bearing face-bridging methoxycarbyne ligands, such as $[CuMo_2ClCp_2(\mu\text{-}COMe)(\mu\text{-}PCy_2)(\mu\text{-}CO)]$ (δ_C 330.5 ppm) [7] or $[CuW_2ClCp_2(\mu_3\text{-}COMe)(\mu\text{-}dppm)(CO)_2]BF_4$ (δ_C 332.7 ppm) [39b].

Spectroscopic data in solution for **9**, however, are not conclusive concerning the question of whether the dimeric structure found in the crystal is retained in solution or not. The fact that Cu–Cl lengths in the crystal differ by 0.1 Å and are in turn significantly longer than those of terminal Cu–Cl bonds suggests that splitting into Mo_2CuCl units should be feasible in solution. Moreover, because of the cisoid geometry of these subunits, any recombination in solution should yield two different diastereoisomers in similar amounts, a circumstance not observed. Based on these considerations, we trust that compound **9** exists in solution as discrete Mo_2Cu clusters, although retention of the dimeric structure found in the crystal cannot be completely ruled out.

3. Conclusions

The benzylidyne-bridged complexes **1** and **2** are nucleophilic enough to react with different metal complexes able to act as precursors of unsaturated $M(CO)_n$ and ML fragments, to give a wide variety of electronically unsaturated heterometallic clusters with Mo_2M triangular cores triply-bridged by the benzylidyne ligand (M = W, Fe, Ru, Au, Cu) or with tetrahedral Mo_2Co_2 cores. The dicarbonyl complex **2** proved to be more active in these reactions, thanks to its more accessible, if less unsaturated, dimetal centre, but almost all the new heterometallic clusters formed are more stable with a cisoid arrangement of their $Mo_2Cp_2(CO)_2$ subunits (as opposed to the transoid arrangement in **2**), presumably because this allows for a more tight binding in the Mo_2MC tetrahedral core supporting these products. When compared to their related methoxycarbyne-bridged complexes, the benzylidyne complex **1** displayed a lower activity in these cluster-building reactions, perhaps resulting from the higher steric requirements of the benzylidyne (vs. COMe) ligand. In contrast, the less hindered dicarbonyl **2** yielded Mo_2Au and Mo_2Cu derivatives which are not accessible by starting from the corresponding methoxycarbyne-bridged analogue, this possibly reflecting the higher electron density at the benzylidyne C atom. Otherwise, the behaviour of compounds **1** and **2** in these reactions can be described as comparable to that of their methoxycarbyne-bridged analogues.

4. Experimental

All reactions and manipulations were carried out under a nitrogen atmosphere using standard Schlenk techniques. Solvents were purified according to literature procedures [40], and distilled under nitrogen prior to use. Petroleum ether refers to that fraction distilling in the range 338-343 K. Complexes $[Mo_2Cp_2(\mu\text{-CPh})(\mu\text{-PCy}_2)(\mu\text{-CO})]$ (**1**) and $[Mo_2Cp_2(\mu\text{-CPh})(\mu\text{-PCy}_2)(CO)_2]$ (**2**) (Cp = η^5-C_5H_5) were prepared as described previously [3]. All other reagents were obtained from the usual commercial suppliers and used as received. Photochemical experiments were performed using jacketed quartz or Pyrex Schlenk tubes, cooled by tap water (ca. 288 K) unless otherwise stated. A 400 w mercury lamp placed ca. 1 cm away from the Schlenk tube was used for all experiments. Chromatographic separations were carried out using jacketed columns cooled by tap water (ca. 288 K) or by a closed 2-propanol circuit kept at the desired temperature with a cryostat. Commercial aluminium oxide (activity I, 70-290 mesh) was degassed under vacuum prior to use. The later was mixed under nitrogen with the appropriate amount of water to reach the activity desired. IR stretching frequencies of CO ligands were measured either in solution (using CaF_2 windows) or in Nujol mulls (using NaCl windows), are referred to as ν(CO) and are given in cm^{-1}. Nuclear magnetic

resonance (NMR) spectra were routinely recorded at 400.13 (^{1}H), 161.97 (^{31}P{^{1}H}) and 100.61 MHz (^{13}C{^{1}H}) at 290 K in CD_2Cl_2 solutions unless otherwise stated. Chemical shifts (δ) are given in ppm, relative to internal tetramethylsilane (^{1}H and ^{13}C), and external 85% aqueous H_3PO_4 solutions (^{31}P). Coupling constants (J) are given in Hertz.

*4.1. Preparation of [$Mo_2FeCp_2(\mu_3$-CPh)(μ-PCy_2)$(CO)_5$] (**3a**).*

Solid [$Fe_2(CO)_9$] (0.035 g, 0.096 mmol) was added to a toluene solution (10 mL) of compound **1** (0.050 g, 0.078 mmol), and the mixture was stirred at room temperature for 5 h to give a green solution. The solvent was then removed under vacuum, the residue extracted with petroleum ether and the extracts chromatographed through an alumina column (activity IV). Elution with dichloromethane/petroleum ether (1/8) gave a greenish-grey fraction yielding, after removal of solvents under vacuum, compound **3a** as a green microcrystalline solid (0.056 g, 89%). The crystals used in the X-ray study were grown by the slow diffusion of a layer of petroleum ether into a dichloromethane solution of the complex at 253 K. Anal. Calc. for $C_{34}H_{37}FeMo_2O_5P$: C, 50.77; H, 4.64. Found: C, 50.28; H, 4.70. ^{1}H NMR: δ 7.30-7.12 (m, br, 3H, Ph), 7.04 [m, br, 2H, H^{2}(Ph)], 4.95 (s, 10H, Cp), 2.63-1.27 (m, 22H, Cy). ^{1}H NMR (233 K): δ 8.54 [d, J_{HH} = 7, 1H, H^{2}(Ph)], 7.43 [t, J_{HH} = 7, 1H, H^{4}(Ph)], 7.08 [m, 2H, H^{3}(Ph)], 5.40 [s, br, 1H, H^{2}(Ph)], 4.98 (s, 10H, Cp), 2.60-1.27 (m, 22H, Cy). ^{13}C{^{1}H} NMR: δ 306.9 (s, μ_3-C), 249.8 (d, J_{CP} = 7, MoCO), 217.3 (s, 3FeCO), 165.6 [s, C^{1}(Ph)], 127.7 [s, C^{3+4}(Ph)], 125.6 [s, C^{2}(Ph)], 91.3 (s, Cp), 50.0 [d, J_{CP} = 24, C^{1}(Cy)], 44.5 [d, J_{CP} = 15, C^{1}(Cy)], 34.4, 33.0 [2s, C^{2}(Cy)], 28.2 [d, J_{CP} = 10, 2C^{3}(Cy)], 26.6 [s, 2C^{4}(Cy)].

*4.2. Preparation of [$Mo_2RuCp_2(\mu_3$-CPh)(μ-PCy_2)$(CO)_5$] (**3b**).*

Solid [$Ru_3(CO)_{12}$] (0.050 g, 0.078 mmol) was added to a tetrahydrofuran solution (10 mL) of compound **1** (0.050 g, 0.078 mmol), and the mixture was irradiated with visible-UV light in a Pyrex Schlenk flask for 20 min, while keeping a gentle N_2 purge, to give a green solution. Workup as described for **3**a yielded compound **3b** as a green solid (0.059 g, 89%). Anal. Calc. for $C_{34}H_{37}Mo_2O_5PRu$: C, 48.07; H, 4.39. Found: C, 47.68; H, 4.52. ^{1}H NMR: δ 7.13 [m, br, J_{HH} = 7, 2H, H^{3}(Ph)], 6.96 [t, J_{HH} = 7, 1H, H^{4}(Ph)], 4.97 (s, 10H, Cp), 2.68 (m, 1H, Cy), 2.14-1.18 (m, 21H, Cy). ^{1}H NMR (183 K): δ 8.38 [d, J_{HH} = 7, 1H, H^{2}(Ph)], 7.36 [t, J_{HH} = 7, 1H, H^{4}(Ph)], 7.00 [m, 2H, H^{3}(Ph)], 5.42 (s, 10H, Cp), 5.30 [d, J_{HH} = 7, 1H, H^{2}(Ph)], 2.82 (m, 1H, Cy), 2.12-1.22 (m, 21H, Cy). ^{13}C{^{1}H} NMR: δ 286.7 (s, μ_3-C), 253.0 (d, J_{CP} = 7, MoCO), 201.8 (s, 3RuCO), 165.6 [s, C^{1}(Ph)], 128.2 [s, C^{3}(Ph)], 127.6 [s, C^{4}(Ph)], 125.2 [s, C^{2}(Ph)], 90.8 (s, Cp), 49.4 [d, J_{CP} = 22, C^{1}(Cy)], 44.2 [d, J_{CP} = 15, C^{1}(Cy)], 34.5, 32.8 [2s, C^{2}(Cy)], 28.3 [d, J_{CP} = 11, 2C^{3}(Cy)], 26.7 [s, 2C^{4}(Cy)].

*4.3. Preparation of [$Co_2Mo_2Cp_2(\mu_3$-CPh)(μ-PCy_2)$(CO)_7$] (**4**).*

Solid [$Co_2(CO)_8$] (0.035 g, 0.102 mmol) was added to a toluene solution (10 mL) of compound **1** (0.050 g, 0.078 mmol), and the mixture was stirred at room temperature for 1 h to give a brown solution. The solvent was then removed under vacuum, the residue extracted with dichloromethane/petroleum ether (1/10) and the extracts chromatographed through an alumina column (activity IV). Elution with dichloromethane/petroleum ether (1/1) gave a brown fraction yielding, after removal of solvents, compound **4** as a brown microcrystalline solid (0.065 g, 90%). Anal. Calc. for $C_{36}H_{37}Co_2Mo_2O_7P$: C, 46.88; H, 4.04. Found: C, 46.52; H, 4.21. Compound **4** displays in solution two isomers (**A** and **B**) only detectable at low temperature (ratio **A**/**B** ca. 2/1 at 183 K). IR (toluene): ν(CO) 2014 (s), 1983 (vs), 1975 (sh), 1886 (w), 1859 (w), 1827 (w), 1764 (w). ^{1}H NMR: δ 7.34 [false t, J_{HH} = 7, 2H, H^3(Ph)], 7.33 [false d, J_{HH} = 7, 2H, H^2(Ph)], 7.14 [t, J_{HH} = 7, 1H, H^4(Ph)], 5.27, 4.90 (2s, 2 × 5H, Cp), 2.62 (m, 1H, Cy), 2.40 (m, 1H, Cy), 2.20-1.15 (m, 20H, Cy). ^{13}C{^{1}H} NMR: δ 167.8 [s, C^1(Ph)], 128.1 [s, C^3(Ph)], 125.7 [s, C^2(Ph)], 125.5 [s, C^4(Ph)], 98.8, 92.2 (2s, Cp), 54.1, 51.6 [2s, br, 2C^1(Cy)], 34.6, 34.1 [2d, J_{CP} = 2, C^2(Cy)], 32.1, 32.0 [2s, C^2(Cy)], 28.4, 28.4, 28.2, 28.1 [4d, J_{CP} = 10, C^3(Cy)], 26.6, 26.4 [2s, C^4(Cy)]. The carbonyl resonances could not be identified in this spectrum. *Isomer **A***: ^{31}P{^{1}H} NMR (183 K): δ 316.9. ^{1}H NMR (183 K): δ 7.48-7.00 (m, 5H, Ph), 5.38, 5.17 (2s, 2 × 5H, Cp), 2.59-1.00 (m, 22H, Cy). ^{13}C{^{1}H} NMR (183 K): δ 309.3 (s, μ_3-C), 273.8, 257.0, 243.6, 230.6 (4s, MoCO and μ-CO), 210.3, 206.1 (br), 204.2 (3s, CoCO), 165.9 [s, C^1(Ph)], 128.0, 126.8, 126.2 (3s, Ph), 98.4, 92.0 (2s, Cp), 54.1, 51.6 [2s, br, C^1(Cy)], 34.6, 33.0, 32.3, 30.7 [4s, C^2(Cy)], 28.0 [s, br, C^3(Cy)], 26.4, 26.2 [2s, C^4(Cy)]. *Isomer **B***: ^{31}P{^{1}H} NMR (183 K): δ 347.2. ^{1}H NMR (183 K): δ 7.48-7.00 (m, 5H, Ph), 5.31, 4.70 (2s, 2 × 5H, Cp), 2.59-1.00 (m, 22H, Cy). ^{13}C{^{1}H} NMR (183 K): δ 272.7, 253.5, 245.4, (3s, MoCO and μ-CO), 207.0 (br), 200.0 (2s, CoCO), 165.9 [s, C^1(Ph)], 128.3 (s, Ph), 99.5, 92.2 (2s, Cp); other resonances of the minor isomer **B** could not be clearly identified in the spectrum.

*4.4. Preparation of [$Co_2Mo_2Cp_2(\mu_3$-CPh)(μ-PCy$_2$)(CO)$_4$(μ-CO)$_3$] (**5**).*

A solution of compound **4** (0.060 g, 0.065 mmol) in toluene (10 mL) was stirred at room temperature for 10 h (or heated at 243 K for 3 h) to give a brown solution. After removal of the solvent under vacuum, the residue was washed with petroleum ether (2 × 3 mL) to give compound **5** as a brown powder (0.057 g, 95 %). The crystals used in the X-ray study were grown by the slow diffusion of a layer of petroleum ether into a dichloromethane solution of the complex at 253 K. Anal. Calc. for $C_{37}H_{39}Cl_2Co_2Mo_2O_7P$ (**5**·CH_2Cl_2): C, 44.12; H, 3.90. Found: C, 44.06; H, 4.10. IR (nujol): ν(CO) 2004 (s), 1975 (vs), 1968 (s), 1900 (s), 1824 (w), 1784 (w), 1764 (s). ^{1}H NMR (298 K): δ 7.38 [s, br, 4H, H^{2+3}(Ph)], 7.13 [s, br, 1H, H^4(Ph)], 5.00 (s, 10H, Cp), 2.10-1.30 (m, 22H, Cy). ^{13}C{^{1}H} NMR (298 K): δ 302.4 (d, J_{CP} = 18, μ_3-C), 256.8 (s, br, CO), 204.6 (s, br, CO), 167.9 [s, C^1(Ph)], 128.1 [s, C^3(Ph)], 127.4 [s, C^4(Ph)], 125.7

[s, C^2(Ph)], 97.2 (s, br, Cp), 51.6 [s, br, C^1(Cy)], 33.4, 32.2 [2s, br, C^2(Cy)], 28.4, 28.3 [2s, C^3(Cy)], 26.4 [s, 2C^4(Cy)]. $^{31}P\{^1H\}$ NMR (183 K): δ 383.4. ^1H NMR (183 K): δ 7.58 [s, br, 1H, H^4(Ph)], 7.41 [s, br, 2H, H^3(Ph)], 7.20 [s, br, 2H, H^2(Ph)], 5.19, 4.88 (2s, 2 × 5H, Cp), 2.77-1.26 (m, 22H, Cy). $^{13}C\{^1H\}$ NMR (183 K): δ 302.6 (s, μ_3-C), 262.7, 254.3, 249.8, 230.0 (4s, MoCO and μ-CO), 208.2, 205.0, 199.6 (3s, CoCO), 167.2 [s, C^1(Ph)], 129.1, 128.6, 127.9, 125.6, 125.1 (5s, Ph), 99.7, 94.7 (2s, Cp), 56.1, 47.0 [2s, br, C^1(Cy)], 34.6, 34.2, 31.3, 29.3 [4s, br, C^2(Cy)], 28.0 [s, br, 4C^3(Cy)], 26.0 [s, 2C^4(Cy)].

*4.5. Preparation of [$Mo_2WCp_2(\mu_3$-CPh)(μ-PCy_2)$(CO)_6$] (**6**).*

A toluene solution containing compound **2** (0.050 g, 0.075 mmol) and [$W(CO)_6$] (0.050 g, 0.142 mmol) was irradiated with visible-UV light in a quartz Schlenk flask at 263 K for 90 min with a gentle N_2 purge to give a brown solution. The solvent was then removed under vacuum. The residue contained a mixture of the isomers ***cis*-6** and ***trans*-6** in a ratio of 5/4, along with variable amounts of the known complexes **1** and its ketenyl derivative [Mo_2Cp_2{μ-C(O)Ph}(μ-PCy_2)$(CO)_2$]. All attempts to further purify compound **6** resulted in its progressive decomposition to give compound **1** and [$W(CO)_6$]. *Spectroscopic data for **cis*-6***: ^1H NMR (233 K): δ 7.53 [t, J_{HH} = 7, 1H, H^4(Ph)], 7.05 [false t, J_{HH} = 7, 2H, H^3(Ph)], 6.62 [false d, J_{HH} = 7, 2H, H^2(Ph)], 4.98 (s, 10H, Cp), 2.61-0.90 (m, 22H, Cy). $^{13}C\{^1H\}$ NMR (233 K): δ 300.5 (s, μ_3-C), 222.7 (s, br, MoCO), 166.5 [s, C^1(Ph)], 130.2 [s, C^4(Ph)], 129.9 [s, C^3(Ph)], 127.8 [s, C^2(Ph)], 91.3 (s, Cp), 49.8 [d, J_{CP} = 20, C^1(Cy)], 48.5 [d, J_{CP} = 26, C^1(Cy)], 34.2 [s, C^2(Cy)], 32.8 [d, J_{CP} = 2, C^2(Cy)], 28.2 [d, J_{CP} = 12, C^3(Cy)], 27.9 [d, J_{CP} = 11, C^3(Cy)], 26.5, 26.4 [2s, 2C^4(Cy)]. *Spectroscopic data for **trans*-6***: ^1H NMR (233 K): δ 5.60, 5.34 (2s, 2 × 5H, Cp), 2.61-0.90 (m, 22H, Cy); the phenyl resonances of this isomer were obscured by those of residual toluene, which could not be efficiently removed from the mixture without causing extensive decomposition on compound **6**. $^{13}C\{^1H\}$ NMR (233 K): δ 162.2 [s, C^1(Ph)], 128.5 [s, C^3(Ph)], 125.6 [s, C^4(Ph)], 124.8 [s, C^2(Ph)], 90.4, 88.9 (2s, Cp), 42.0 [d, J_{CP} = 20, C^1(Cy)], 40.7 [d, J_{CP} = 19, C^1(Cy)], 35.0 [d, J_{CP} = 1, C^2(Cy)], 33.4, 33.2, 32.4 [3s, C^2(Cy)], 28.2 [d, J_{CP} = 12, 2C^3(Cy)], 28.1 [d, J_{CP} = 11, C^3(Cy)], 27.3 [d, J_{CP} = 10, C^3(Cy)], 26.0, 25.9 [2s, C^4(Cy)]. The W-bound CO resonances could not be clearly identified in the spectrum of the crude reaction mixture.

*4.6. Preparation of trans-[$AuMo_2Cp_2(\mu_3$-CPh)(μ-PCy_2)$(CO)_2(PMe_3)](PF_6)$ (**7a**).*

Dichloromethane (10 mL) was added to a mixture of compound **2** (0.050 g, 0.075 mmol), [$AuCl(PMe_3)$] (0.025 g, 0.081 mmol) and $TlPF_6$ (0.026 g, 0.075 mmol), and the mixture was stirred for 1 h to give a red-brown solution. After removal of the solvent under vacuum, the residue was extracted with dichloromethane/petroleum ether (1/1) and the extracts chromatographed through an alumina column (activity IV) at 253 K.

Elution with dichloromethane/tetrahydrofuran (9/1) gave a single brown fraction yielding, after removal of solvents under vacuum, compound **7a** as a brown oil (0.060 g, 74%). ^{1}H NMR (233 K): δ 7.66 [false t, J_{HH} = 8, 2H, H^3(Ph)], 7.50 [false d, J_{HH} = 7, 2H, H^2(Ph)], 7.41 [t, J_{HH} = 7, 1H, H^4(Ph)], 5.72, 5.26 (2s, 2 × 5H, Cp), 2.60-0.80 (m, 22H, Cy), 1.32 (d, J_{HP} = 11, 9H, PMe]. ^{13}C{^{1}H} NMR: δ 377.0 (d, J_{CP} = 25, μ_3-C), 232.6 (s, MoCO), 225.3 (d, J_{CP} = 11, MoCO), 164.0 [s, C^1(Ph)], 129.2 [s, C^4(Ph)], 128.9 [s, C^3(Ph)], 124.7 [s, C^2(Ph)], 92.5, 91.0 (2s, Cp), 52.8 [d, J_{CP} = 20, C^1(Cy)], 42.2 [d, J_{CP} = 14, C^1(Cy)], 35.3, 34.3 [2d, J_{CP} = 3, C^2(Cy)], 34.2, 33.3 [2s, C^2(Cy)], 28.3 [d, J_{CP} = 12, C^3(Cy)], 28.2, 28.1 [2d, J_{CP} = 10, C^3(Cy)], 28.0 [d, J_{CP} = 12, C^3(Cy)], 26.3, 26.1 [2s, C^4(Cy)], 15.8 (d, J_{CP} = 36, PMe).

*4.7. Preparation of trans-[AuMo$_2$Cp$_2$(μ_3-CPh)(μ-PCy$_2$)(CO)$_2${P(p-tol)$_3$}](PF$_6$) (**7b**).*

The procedure is identical to that described for **7a**, but using [AuCl{P(*p*-tol)$_3$}] (0.050 g, 0.093 mmol) instead of [AuCl(PMe$_3$)]. After similar workup, compound **7b** was isolated as a brown oil (0.075 g, 76%). ^{1}H NMR (300.09 MHz): δ 7.42-7.10 [m, 14H, C$_6$H$_4$ and H^3(Ph)], 6.94 [t, J_{HH} = 7, 1H, H^4(Ph)], 6.83 [false d, J_{HH} = 7, 2H, H^2(Ph)], 5.54, 5.45 (2s, 2 × 5H, Cp), 2.50-0.90 (m, 22H, Cy), 2.44 (s, 9H, Me).

*4.8. Preparation of trans-[AuMo$_2$Cp$_2$(μ_3-CPh)(μ-PCy$_2$)(CO)$_2$(P^{i}Pr$_3$)](PF$_6$) (**7c**).*

The procedure is identical to that described for **7a**, but using [AuCl(P^{i}Pr$_3$)] (0.030 g, 0.075 mmol) instead of [AuCl(PMe$_3$)]. After similar workup, compound **7c** was isolated as a brown oil (0.072 g, 82%). ^{1}H NMR (233 K): δ 7.65 [false t, J_{HH} = 7, 2H, H^3(Ph)], 7.56 [false d, J_{HH} = 7, 2H, H^2(Ph)], 7.43 [t, J_{HH} = 7, 1H, H^4(Ph)], 5.66, 5.37 (2s, 2 × 5H, Cp), 2.50-1.00 (m, 22H, Cy), 2.12 (d sept, J_{HP} = 8, J_{HH} = 7, 3H, C*H*Me$_2$], 1.01, 1.00 (2dd, J_{HP} = 16, J_{HH} = 7, 2 × 6H, Me). ^{13}C{^{1}H} NMR (233 K): δ 370.0 (d, J_{CP} = 19, μ_3-C), 234.2 (s, br, MoCO), 227.1 (d, J_{CP} = 11, MoCO), 161.6 [s, C^1(Ph)], 129.8 [s, C^4(Ph)], 128.9 [s, C^3(Ph)], 126.0 [s, C^2(Ph)], 92.5, 91.7 (2s, Cp), 52.7 [d, J_{CP} = 18, C^1(Cy)], 47.7 [d, J_{CP} = 17, C^1(Cy)], 35.1 [d, J_{CP} = 3, C^2(Cy)], 34.5 [s, C^2(Cy)], 34.3, 34.2 [2s, br, C^2(Cy)], 28.3 [d, J_{CP} = 12, 2C^3(Cy)], 28.2 [d, J_{CP} = 11, 2C^3(Cy)], 26.2, 26.1 [2s, C^4(Cy)], 24.1 [d, J_{CP} = 28, *C*HMe$_2$], 19.9 (s, 2Me).

*4.9. Preparation of cis-[AuMo$_2$Cp$_2$(μ_3-CPh)(μ-PCy$_2$)(CO)$_2$(PMe$_3$)](PF$_6$) (**8a**).*

A solution of compound **7a** (0.060 g, 0.055 mmol) in dichloromethane (10 mL) stirred at room temperature for 5 h evolved quantitatively to give a mixture of the isomers ***syn*-8a** and ***anti*-8a** in a 1/5 ratio. Removal of the solvent under vacuum and washing of the residue with petroleum ether (3 mL) yielded compound **8a** as a red-brown solid (0.055 g, 92%). Anal. Calc. For C$_{34}$H$_{46}$AuF$_6$Mo$_2$O$_2$P$_3$: C, 37.73; H, 4.28. Found: C, 37.56; H, 4.20. *Spectroscopic data for isomer **anti-8a***: ^{1}H NMR: δ 7.34 [false t, J_{HH} = 7, 2H, H^3(Ph)], 7.05 [t, J_{HH} = 7, 1H, H^4(Ph)], 6.44 [false d, J_{HH} = 7, 2H,

H^2(Ph)], 5.53 (s, 10H, Cp), 3.72 (m, 1H, Cy), 2.60-0.90 (m, 19H, Cy), 1.50 (d, J_{HP} = 10, 9H, PMe], 0.17 (m 2H, Cy). $^{13}C\{^1H\}$ NMR: δ 348.3 (d, J_{CP} = 26, μ_3-C), 228.4 (d, J_{CP} = 10, MoCO), 165.1 [s, C^1(Ph)], 128.1 [s, C^3(Ph)], 127.9 [s, C^4(Ph)], 118.0 [s, C^2(Ph)], 93.9 (s, Cp), 53.4 [d, J_{CP} = 25, C^1(Cy)], 44.7 [d, J_{CP} = 6, C^1(Cy)], 34.7 [d, J_{CP} = 4, C^2(Cy)], 33.3 [s, C^2(Cy)], 28.7, 27.4 [2d, J_{CP} = 12, C^3(Cy)], 26.6, 26.2 [2s, C^4(Cy)], 15.4 (d, J_{CP} = 35, PMe). *Spectroscopic data for isomer* ***syn-8a***: ^1H NMR: δ 7.50 [false t, J_{HH} = 7, 2H, H^3(Ph)], 7.09 [t, J_{HH} = 7, 1H, H^4(Ph)], 6.83 [false d, J_{HH} = 7, 2H, H^2(Ph)], 5.33 (s, 10H, Cp), 3.92 (m, 1H, Cy), 2.60-0.90 (m, 19H, Cy), 1.60 (d, J_{HP} = 10, 9H, PMe], 0.17 (m 2H, Cy). $^{13}C\{^1H\}$ NMR: δ 233.5 (d, J_{CP} = 10, MoCO), 162.5 [s, C^1(Ph)], 125.5 [s, C^4(Ph)], 124.9 [s, C^3(Ph)], 121.1 [s, C^2(Ph)], 94.2 (s, Cp), 51.8 [d, J_{CP} = 25, C^1(Cy)], 47.2 [d, J_{CP} = 10, C^1(Cy)], 34.3 [d, J_{CP} = 4, C^2(Cy)], 32.9 [s, C^2(Cy)], 28.5, 27.4 [2d, J_{CP} = 12, C^3(Cy)], 26.2, 26.0 [2s, C^4(Cy)], 15.4 (d, J_{CP} = 35, PMe); the carbyne resonance of this minor isomer could not be identified in the spectrum.

*4.10. Preparation of cis-[$AuMo_2Cp_2(\mu_3$-CPh)(μ-PCy_2)$(CO)_2${P(p-tol)$_3$}](PF$_6$) (**8b**).*

A solution of compound **7b** (0.075 g, 0.057 mmol) in dichloromethane (10 mL) stirred at room temperature for 7 h evolved quantitatively to give compound **8b** as the unique product. Removal of solvent under vacuum and washing of the residue with petroleum ether (3 mL) yielded compound **8b** as a red-brown solid (0.070 g, 93%). Anal. Calc. for $C_{52}H_{58}AuF_6Mo_2O_2P_3$: C, 47.65; H, 4.46. Found: C, 47.45, H, 4.37. ^1H NMR: δ 7.40-7.12 [m, 14H, C_6H_4 and H^3(Ph)], 7.05 [t, J_{HH} = 7, 1H, H^4(Ph)], 6.50 [false d, J_{HH} = 7, 2H, H^2(Ph)], 5.50 (s, 10H, Cp), 2.50-0.90 (m, 19H, Cy), 2.40 (s, 9H, Me), 0.12 (m, 2H, Cy).

*4.11. Preparation of cis-[$AuMo_2Cp_2(\mu_3$-CPh)(μ-PCy_2)$(CO)_2(P^iPr_3)$](PF$_6$) (**8c**).*

A solution of compound **7c** (0.070 g, 0.060 mmol) in dichloromethane (10 mL) stirred at room temperature for 18 h evolved quantitatively to give compound **8c** as the unique product. Removal of solvent under vacuum and washing of the residue with petroleum ether (3 mL) yielded compound **8c** as a purple-brown solid (0.065 g, 92%). Anal. Calc. for $C_{40}H_{58}AuF_6Mo_2O_2P_3$: C, 41.18; H, 5.01. Found: C, 40.92; H, 4.88. Good-quality crystals of the complex were very difficult to obtain; the crystals used in the X-ray study were grown by the slow diffusion of a layer of petroleum ether into a tetrahydrofuran solution of the complex at 253 K, but the single crystal used for data adquisition turned to be the double salt $[AuMo_2Cp_2(\mu_3$-CPh)(μ-PCy_2)$(CO)_2(P^iPr_3)]_2(PF_6)(Cl)\cdot$1/2THF, possibly formed due to the presence of residual chloride ions in the solution of the complex. ^1H NMR: δ 7.34 [false t, J_{HH} = 7, 2H, H^3(Ph)], 7.09 [t, J_{HH} = 7, 1H, H^4(Ph)], 6.58 [false d, J_{HH} = 7, 2H, H^2(Ph)], 5.49 (s, 10H, Cp), 3.96 (m, 1H, Cy), 2.60-0.90 (m, 19H, Cy), 2.41 (d sept, J_{HP} = 8, J_{HH} = 7, 3H, C*H*Me_2], 1.19 (dd, J_{HP} = 16, J_{HH} = 7, 18H, Me), 0.12 (m, 2H, Cy). $^{13}C\{^1H\}$ NMR: δ

346.6 (d, J_{CP} = 25, μ_3-C), 230.4 (d, J_{CP} = 10, MoCO), 165.1 [s, C^1(Ph)], 128.1 [s, C^3(Ph)], 125.2 [s, C^4(Ph)], 118.2 [s, C^2(Ph)], 94.1 (s, Cp), 53.0 [d, J_{CP} = 25, C^1(Cy)], 45.3 [d, J_{CP} = 7, C^1(Cy)], 34.7 [d, J_{CP} = 4, C^2(Cy)], 33.2 [s, C^2(Cy)], 28.7 [d, J_{CP} = 12, C^3(Cy)], 27.3 [d, J_{CP} = 11, C^3(Cy)], 26.6, 26.2 [2s, C^4(Cy)], 24.8 [d, J_{CP} = 26, *C*HMe_2], 20.1 (s, Me).

*4.12. Preparation of [$CuMo_2ClCp_2(\mu_3$-CPh)(μ-PCy_2)$(CO)_2$] (**9**).*

Solid CuCl (0.010 g, 0.101 mmol) was added to a dichloromethane solution (5 mL) of compound **2** (0.050 g, 0.075 mmol), and the mixture was stirred at room temperature for 30 min to give a purple solution. The solvent was then removed under vacuum, the residue extracted with dichloromethane/petroleum ether (1/1) and the extracts were chromatographed through an alumina column (activity IV) at 253 K. Elution with dichloromethane/tetrahydrofuran (9/1) gave a purple fraction yielding, after removal of solvents, compound **9** as a violet microcrystalline solid (0.045 g, 78%). The crystals used in the X-ray study were grown by the slow diffusion of a layer of petroleum ether into a dichloromethane solution of the complex at 253 K. Anal. Calc. for $C_{31}H_{37}CuClMo_2O_2P$: C, 48.77; H, 4.88. Found: C, 48.55; H, 4.52. IR (nujol): ν(CO) 1920 (vs), 1864 (w). ^{1}H NMR (300.13 MHz): δ 7.30 [false t, J_{HH} = 8, 2H, H^3(Ph)], 7.00 [t, J_{HH} = 8, 1H, H^4(Ph)], 6.54 [false d, J_{HH} = 8, 2H, H^2(Ph)], 5.41 (s, 10H, Cp), 3.39 (m, 1H, Cy), 2.65-0.12 (m, 21H, Cy). $^{13}C\{^1H\}$ NMR: δ 349.2 (s, μ_3-C), 224.9 (d, J_{CP} = 10, MoCO), 169.4 [s, C^1(Ph)], 127.8 [s, C^4(Ph)], 123.8 [s, C^3(Ph)], 118.7 [s, C^2(Ph)], 93.6 (s, Cp), 51.2 [d, J_{CP} = 26, C^1(Cy)], 43.3 [d, J_{CP} = 8, C^1(Cy)], 35.2 [d, J_{CP} = 4, C^2(Cy)], 33.7 [s, C^2(Cy)], 28.8 [d, J_{CP} = 11, C^3(Cy)], 27.6 [d, J_{CP} = 12, C^3(Cy)], 26.8, 26.4 [2s, C^4(Cy)].

*4.13. X-ray Data Collection, Structure Determination and Refinements for Compounds **3a**, **5**, **8c** and **9**.*

The X-ray intensity data for compounds **3a**, **5** and **9** were collected on a Kappa-Appex-II Bruker diffractometer using graphite-monochromated MoK_α radiation at 100 K. The software APEX was used for collecting frames with the ω/ϕ scans measurement method [41]. The Bruker SAINT software was used for data reduction [42], and a multi-scan absorption correction was applied with SADABS [43]. Using the program suite WinGX [44], the structures were solved by Patterson interpretation and phase expansion using SHELXL97 [45], and refined with full-matrix least squares on F^2 using SHELXL97. All hydrogen atoms were geometrically placed and refined using a riding model, and all positional parameters and anisotropic temperature factors for all non-H atoms were anisotropically refined in general. Two independent molecules, very similar to each other, were present in the asymmetric unit of compound **3a**. Compound **9** crystallized with two molecules of dichloromethane, and the molecule of complex was

placed on the symmetry operation −x,−y+1,−z+1. Compound **5** crystallized with a molecule of dichloromethane and one of the cyclohexyl groups was found to be disordered over two positions, satisfactorily refined with 0.6/0.4 occupancies. The carbon atoms involved in disorder were refined isotropically to prevent their temperature factors from becoming non-positive definite.

Data collection for compound **8c** was performed at 150 K on an Oxford Diffraction Xcalibur Nova single crystal diffractometer, using CuK_α radiation. Images were collected at a 70 mm fixed crystal-detector distance, using the oscillation method, with 1º oscillation and variable exposure time per image (12-45 s). Data collection strategy was calculated with the program CrysAlis Pro CCD [46]. Data reduction and cell refinement was performed with the program CrysAlis Pro RED [46], an empirical absorption correction was applied using the SCALE3 ABSPACK algorithm as implemented in the latter program. Structure solution and refinements were performed as described above. This complex crystallized with half a molecule of tetrahydrofuran, placed on the symmetry element –x,1/2–y,1/2+z, and with two different anions, PF_6^- and Cl^-, placed in parallel and alternating planes, thus yielding and overall stoichiometry $[AuMo_2Cp_2(\mu_3\text{-}CPh)(\mu\text{-}PCy_2)(CO)_2(P^iPr_3)]_2(PF_6)(Cl)\cdot THF$. Moreover, one cyclopentadienyl ligand and one isopropyl group of the cation were found to be disordered. The first disorder was satisfactorily modelled over two sites with 0.5 occupancies, but disorder in the isopropyl group could not be satisfactorily modelled. Due to low quality of the diffraction data, not all non-H atoms could be freely refined anisotropically. A certain number had to be refined anisotropically in combination with the instructions DELU and SIMU and some restraints had to be applied to a few interatomic distances, still one of the carbon atoms had to be refined isotropically to prevent its temperature factors from becoming non positive definite. Yet, some unidentified electron density was still present in the asymmetric unit. To improve this, the SQUEEZE procedure [47], as implemented in PLATON [48], was used. Upon squeeze application and convergence, however, considerable residual electron density remained, with the strongest residual peaks (5.95-3.48 eA^{-3}) being placed close to the metal atoms.

Table 6. Crystal data for new compounds.

	3a	**5**·CH_2Cl_2	**8c**[a]	**9**·CH_2Cl_2
Molecular formula	$C_{34}H_{37}FeMo_2O_5P$	$C_{37}H_{39}Cl_2Co_2Mo_2O_7P$	$C_{84}H_{124}Au_2ClF_6Mo_4O_5P_5$	$C_{64}H_{78}Cl_6Cu_2Mo_4O_4P_2$
Molecular weight	804.34	1007.29	2295.83	1696.76
Crystal system	Monoclinic	Monoclinic	Orthorhombic	Monoclinic
Space group	*P* 2_1/c	*P* 2_1/c	*C m c a*	*P* 2_1/c
Radiation (λ, Å)	0.71073	0.71073	1.54184	0.71073
a (Å)	17.7449(8)	9.9346(11)	55.3156(13)	15.2300(4)
b (Å)	18.4550(9)	33.805(5)	17.7032(3)	12.2148(3)
c (Å)	20.1418(8)	12.4041(19)	23.4427(4)	17.3452(5)
α (°)	90	90	90	90
β (°)	104.339(2)	117.271(6)	90	94.5400(10)
γ (°)	90	90	90	90
V (Å^3)	6390.6(5)	3702.8(9)	22956.6(8)	3216.63(15)
Z	8	4	8	2
Calculated density (g cm^{-3})	1.672	1.807	1.329	1.752
Absorption coefficient (mm^{-1})	1.312	1.778	9.408	1.751
Temperature (K)	100	100	150	100
θ range (°)	1.18 to 26.02	1.20 to 26.02	3.20 to 73.36	1.34 to 26.02
index ranges (*h*, *k*, *l*)	–21, 21; 0, 22; 0, 24	–12, 10; 0, 41; 0, 15	–64, 68; –21, 16; –28, 26	–18, 18; 0, 15; 0, 21
No of reflns collected	97828	41497	47157	48916
Independent reflections (R_{int})	12592 (0.0672)	7286 (0.0751)	11344 (0.0568)	6314 (0.0762)
Reflections with [$I > 2\sigma(I)$]	9834	5334	10073	4694
R indexes [data with I > 2σ(I)][b]	R_1 = 0.0305, wR_2 = 0.0587[c]	R_1 = 0.0394, wR_2 = 0.0519[d]	R_1 = 0.1112, wR_2 = 0.3006[e]	R_1 = 0.0375, wR_2 = 0.0682[f]
R indexes (all data)[b]	R_1 = 0.0480, wR_2 = 0.0642[c]	R_1 = 0.0690 wR_2 = 0.0604[d]	R_1 = 0.1156, wR_2 = 0.3036[e]	R_1 = 0.0644, wR_2 = 0.0782[f]
Goodness of fit	1.042	1.017	1.044	1.03
No of restraints/parameters	0/775	0/454	28/463	0/370
$\Delta\rho$(max., min.), eÅ^{-3}	0.514 / –0.555	0.679 / –0.590	5.881 / –1.724	0.801 / -0.722

[a] The crystal used corresponded to a double salt of the complex, of formula $[AuMo_2Cp_2(\mu_3\text{-}CPh)(\mu\text{-}PCy_2)(CO)_2(P^iPr_3)]_2(PF_6)(Cl)\cdot THF$. [b] $R_1 = \Sigma||Fo| - |Fc||/\Sigma|Fo|$. $wR_2 = [\Sigma w(|Fo|^2 - |Fc|^2)^2/\Sigma w|Fo|^2]^{1/2}$. $w = 1/[\sigma^2(Fo^2) + (aP)^2 + bP]$ where $P = (Fo^2 + 2Fc^2)/3$. [c] a = 0.0209, b = 5.1088. [d] a = 0.0136, b = 0.0000. [e] a = 0.1532, b = 1090.2080. [f] a = 0.0257, b = 4.8926.

Acknowledgment

We thank the DGI of Spain for financial support (CTQ2012-33187) and the Consejería de Educación of Asturias for a grant (to S.M.). We also thank the X-Ray units of Universidad de Oviedo and Universidad de Santiago de Compostela, Spain, for acquisition of diffraction data.

Author Information

Corresponding author: *****E-mail: mara@uniovi.es

Appendix A. Supplementary Data

CCDC 1415070-1415073 contain the supplementary crystallographic data for compounds **3a**, **5**, **8c** and **9**. These data can be obtained free of charge from The Cambridge Crystallographic Data Centre via www.ccdc.cam.ac.uk/data_request/cif.

References

[1] (a) A. Mayr, H. Hoffmeister, Adv. Organomet. Chem. 32 (1991) 259. (b) H. Fischer, P. Hofmann, F.R. Kreissl, R.R. Shrock, U. Schubert, K. Weiss, Carbyne complexes, VCH Publishers, Weinheim, Germany, 1988. (c) R.J. Angelici, K.P. Heesook, Adv. Organomet. Chem. 27 (1987) 51. (d) F.G.A. Stone, Leaving No Stone Unturned: pathways in organometallic chemistry, American Chemical Society, Washington DC, 1993.

[2] (a) M.E. García, D. García-Vivó, M.A. Ruiz, S. Alvarez, G. Aullón, Organometallics 27 (2007) 4930. (b) M.E. García, D. García-Vivó, M.A. Ruiz, S. Alvarez, G. Aullón, Organometallics 27 (2007) 5912.

[3] M.A. Alvarez, M.E. García, D. García-Vivó, M.E. Martínez, M.A. Ruiz, Organometallics 30 (2011) 2189.

[4] M.A. Alvarez, M.E. García, M.E. Martínez, S. Menéndez, M.A. Ruiz, Organometallics 29 (2010) 710.

[5] M.A. Alvarez, M.E. García, S. Menéndez, M.A. Ruiz, Organometallics 30 (2011) 3694.

[6] F.G.A. Stone, Angew. Chem., Int. Ed. Engl. 23 (1984) 89.

[7] M.E. García, D. García-Vivó, M.A. Ruiz, Organometallics 28 (2009) 4385.

[8] M.A. Alvarez, M.E. García, D. García-Vivó, M.E. Martínez, M.A. Ruiz, Inorg. Chem. 48 (2009) 9767.

[9] M.A. Alvarez, D. García-Vivó, M.E. García, M.E. Martínez, A. Ramos, M.A. Ruiz, Organometallics 27 (2008) 1973.

[10] W.H. Sun, S.H. Yang, H. Q. Wang, Q.F. Zhou, K.B. Yu, J. Organomet. Chem. 465 (1994) 263.

[11] A.J. Bridgeman, M.J. Mays, A.D. Woods, Organometallics 20 (2001) 2076.

[12] P.S. Braterman, Metal Carbonyl Spectra, Academic Press, London, U. K., 1975.

[13] M.J. Mays, P.R. Raithby, K. Sarveswaran, G.A. Solan, J. Chem. Soc., Dalton Trans. (2002) 1671.

[14] M.A. Alvarez, M.E. García, M.E. Martínez, M.A. Ruiz, Organometallics 29 (2010) 904.

[15] M.A. Alvarez, M.E. García, V. Riera, M.A. Ruiz, C. Bois, Y. Jeannin, J. Am. Chem. Soc. 117 (1995) 1324.

[16] (a) M. Green, S.J. Porter, F.G.A. Stone, J. Chem. Soc., Dalton Trans. (1983) 513. (b) M.D. Bermudez, E. Delgado, G.P. Elliot. N.H. Tran-Huy, F. Mayor-Real, F.G.A. Stone, M.J. Winter, J. Chem. Soc., Dalton Trans. (1987) 1235 and references therein. (c) H. Huang, R.P. Hughes, C.R. Landis, A.L. Rheingold. J. Am. Chem. Soc. 128 (2006) 7454.

[17] O. Howarth, in Multinuclear NMR, J. Mason (Ed.), Plenum Press, New York, 1987, Chapter 5.

[18] M.R. Bradford, N.G. Connelly, N.C. Harrison, J.C. Jeffery, Organometallics 8 (1989) 1829.

[19] A.J. Carty, S.A. McLaughin, D. Nucciarone, in Phosphorus-31 NMR Spectroscopy in Stereochemical Analysis, J. G. Verkade, L. D. Quin, (Eds.), VCH, Deerfield Beach, FL, 1987, Chapter 16.

[20] K.H. Theopold, R.G. Bergman, Organometallics 1 (1982) 1571.

[21] R.H. Crabtree, M. Lavin, Inorg. Chem. 25 (1986) 805.

[22] B. Cordero. V. Gómez, A.E. Platero-Prats, M. Revés, J. Echeverría, E. Cremades, F. Barragán, S. Alvarez, Dalton Trans. (2008) 2832.

[23] (a) H. Adams, N.A. Bailey, L.J. Gill, M.J. Morris, F.A. Wildgoose, J. Chem. Soc., Dalton Trans. (1996) 1437. (b) H. Adams, L.V.Y. Guio, M.J. Morris, S.E. Spey. J. Chem. Soc., Dalton Trans. (2002) 2907.

[24] C.M. Alvarez, M.E. García, M.A. Ruiz, Organometallics 23 (2004) 4750.

[25] C.M. Alvarez, M.A. Alvarez, M.E. García, A. Ramos, M.A. Ruiz, C. Graiff, A. Tiripicchio, Organometallics 26 (2007) 321.

[26] M.A. Alvarez, M.E. García, D. García-Vivó, R. Lozano, A. Ramos, M.A. Ruiz, Inorg. Chem. 53 (2014) 11261.

[27] (a) D.G. Evans, D.M.P. Mingos, J. Organomet. Chem. 232 (1982) 171. (b) J.W. Lauher, K.J. Wald, J. Am. Chem. Soc. 103 (1981) 7648.

[28] See for example: R. Carreño, V. Riera, M.A. Ruiz, C. Bois, Y. Jeannin, Organometallics 11 (1992) 2923.

[29] Two-bond couplings increase algebraically with the corresponding angle, and in complexes of the type [MCpXYL$_2$] this yields for $^2J_{XY}$ the general trend $|J_{cis}| > |J_{trans}|$. See, for instance: (a) C. J. Jameson, in Phosphorus-31 NMR Spectroscopy in Stereochemical Analysis, J. G. Verkade, L. D. Quin, (Eds.), VCH, Deerfield Beach, FL, 1987, Chapter 6.

[30] M.A. Alvarez, M.E. García, M.E. Martínez, A. Ramos, M.A. Ruiz, D. Sáez, J. Vaissermann, Inorg. Chem. 45 (2006) 6965.

[31] H. Hartung, B. Walter, U. Baumeister, H.-C. Bottcher, A. Krung, F. Rosche, P.G. Jones, Polyhedron 11 (1992) 1563.

[32] G.A. Carriedo, J.A.K. Howard, F.G.A. Stone, M.J. Went, J. Chem. Soc., Dalton Trans. (1984) 2545.

[33] N. Carr, J.R. Fernández, F.G.A. Stone, Organometallics 10 (1991) 2718.

[34] M.E. García, V. Riera, M.A. Ruiz, M.T. Rueda, D. Sáez, Organometallics 21 (2002) 5515.

[35] M.E. García, D. García-Vivó, M.A. Ruiz, Organometallics 27 (2008) 543.

[36] V.G. Albano, L. Busetto, M.C. Cassini, P. Sabatino, A. Schmitz, V. Zanotti, J. Chem. Soc., Dalton Trans (1995) 2087.
[37] H. Brunner, R. Grassl, J. Wachter, B. Nuber, M.L. Ziegler, J. Organomet. Chem. 393 (1990) 119.
[38] I. Amor, M.E. García, M.A. Ruiz, D. Saez, H. Hamidov, J.C. Jeffery, Organometallics 25 (2006) 4857.
[39] See for example: (a) P.K. Byers, F.G.A. Stone, J. Chem. Soc., Dalton Trans. (1991) 93. (b) M.A. Alvarez, M.E. García, V. Riera, M.A. Ruiz, F. Robert, Organometallics 21 (2002) 1177. (c) J.C. Jeffery, M.A. Ruiz, F.G.A. Stone, J. Organomet. Chem. 355 (1988) 231.
[40] W.L.F. Armarego, C.C.C. Chai, Purification of Laboratory Chemicals, 5th ed., Butterworth-Heinemann, Oxford, U. K., 2003.
[41] APEX 2, version 2.0-1, Bruker AXS Inc, Madison, WI, 2005.
[42] SMART & SAINT Software Reference Manuals, version 5.051 (Windows NT version), Bruker Analytical X-ray Instruments, Madison, WI, 1998.
[43] G.M. Sheldrick, SADABS, Program for Empirical Absorption Correction, University of Göttingen, Göttingen, Germany, 1996.
[44] L.J. Farrugia, J. Appl. Crystallogr. 32 (1999) 837.
[45] G.M. Sheldrick, Acta Crystallogr., Sect. A 64 (2008) 112.
[46] CrysAlis Pro, Oxford Diffraction Ltd., Oxford, U. K., 2006.
[47] P. Van der Sluis, A.L. Spek, Acta Crystallogr., Sect. A 46 (1990) 194.
[48] A.L. Spek, PLATON, A Multipurpose Crystallographic Tool, Utrecht University, Utrecht, The Netherlands, 2010.

For Graphical Abstract Use Only

Synopsis

The title benzylidyne-bridged complexes are nucleophilic enough to react with different metal complexes able to act as precursors of unsaturated $M(CO)_n$ and ML fragments, to give a wide variety of electronically unsaturated heterometallic clusters with Mo_2M triangular cores triply-bridged by the benzylidyne ligand (M = W, Fe, Ru, Au, Cu), or with tetrahedral Mo_2Co_2 cores.

Pictogram for Graphical Abstract

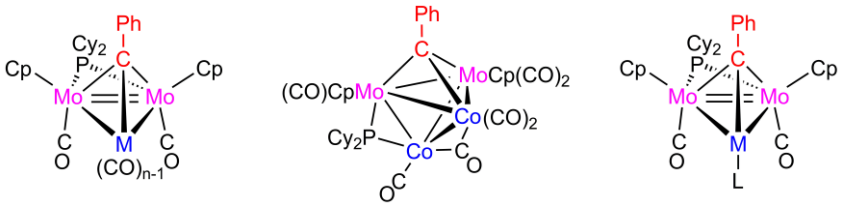

HIGHLIGHTS

- 16-electron $M(CO)_n$ fragments are easily added to the title complexes
- Novel heterometallic clusters are readily synthesized from the title complexes
- Rational synthesis of benzylidyne-bridged clusters from Mo_2 precursors